Elucidating the immunomodulatory properties of small extracellular vesicles derived from SMAC mimetic treated cancer cells

Jordan Jiaxi Yin

A thesis submitted to the University of Ottawa in partial fulfillment of the requirements for the Master's degree in Microbiology and Immunology

Department of Biochemistry, Microbiology and Immunology
Faculty of Medicine
University of Ottawa

Table of Contents

ABSTRACT

Several members of the Inhibitor of Apoptosis (IAP) proteins act as potent anti-apoptotic factors and as key negative regulators of the alternative NF-κB pathway, thereby regulating pro-inflammatory and immune responses. SMAC mimetics (SMs) are a class of drugs designed to antagonize the IAPs, enabling promotion of cell death and stimulation of immune activation. Over the past decade, small extracellular vesicles (sEVs) have gained attention in cancer immunotherapy due to their role in intercellular communication and molecular cargo transfer. This study investigates whether SMs can enhance anti-tumor immune responses mediated by antigen-presenting sEVs. sEVs were isolated from two ovalbumin (OVA)-expressing murine cancer cells, B16F10-OVA and MC38-OVA. The sEVs were characterized using latest MISEV guidelines, such as particle sizing and quantitation, as well as assessment of canonical vesicle-associated markers. The functional capabilities of these sEVs were then evaluated in dendritic cell (DC) co-culture systems to determine their capacity to modulate DC activation, maturation, and antigen presentation. Downstream effects on $CD8^+$ T cell responses were assessed using OT-I T cells as a model of recognizing the OVA-specific priming and activation. My findings support a model in which SMs alter tumour sEV release and immune cell activation. These tumour-derived sEVs alongside with SMs promoted DC activation and OVA antigen presentation. Further, the uptake of tumour-derived sEVs within DCs led to activation of antigen-specific $CD8^+$ T cells, supporting the role of sEV-mediated transfer of both peptide- and immune-relevant signals. Overall, this work identifies how SMs influence adaptive immunity through the context of sEVs. These findings establish a foundation for further investigation into sEV-mediated mechanisms of anti-tumour immunity and support the therapeutic potential of combining SMs with immune-based strategies in cancer.

ACKNOWLEDGEMENTS

I would like to begin by expressing my deepest gratitude to my supervisor, Dr. Shawn Beug, for giving me the opportunity to pursue this research and for supporting my development as both an individual and trainee. I am sincerely thankful for his mentorship, scientific guidance, and encouragement throughout this project. Shawn, thank you for supporting my curiosity, goals, and passions for translational research.

I would also like to extend my appreciation to my sub-supervisor, Dr. Rostyslav Horbay, for his day-to-day guidance and support throughout this thesis. His mentorship in the laboratory, willingness to answer questions (even very late at night), and thoughtful feedback were invaluable to both the progress of this project and my own confidence as a developing scientist. I am grateful for the time and care he dedicated to helping me learn the technical and conceptual aspects of this project. Rostyk, thank you so much for your patience and endless number of ideas for this project.

To Dr. Eric LaCasse, for generously sharing his seemingly encyclopedic knowledge and for always making time to answer my questions. And to my TAC members Dr. Robert Korneluk and Dr. Dylan Burger, for their valuable insights and critiques about my project.

Moreover, I would also like to thank the past and current contributors to this project, Daniel Panting and Maria Dimancheva, whose contributions helped shape the direction and progress of this project. Daniel, thank you for always supporting me in the lab and helping when the big experiments were underway.

I would like to also extend my gratitude towards Nathalie Earl, Kate Daniel, Neena Lala-Tabbert, and Allan Humphrey. Nathalie, thank you so much for being so supportive and always being a listening ear when I needed it. Thank you for also being so patient with my animal training. Kate, thank you for always yapping with me in the lunchroom, crashing out about counting cells,

and chatting about our fitness journeys. Neena and Allan, thank you for always being there if I had any questions about where certain solutions are, how to work machines, and being there for Western advice. Further, I would also like to thank Lynn Kyte for the countless times for helping me with CHEO orders and finding card transaction statements…, and to Martine St-Jean who built the foundation from which I was able to learn and grow.

I would also like to thank the members of the Beug Lab, including Kyle Malone, Mikaela van der Merwe, and Alyssa Tarnocai, for their kindness, advice, and support throughout my time in the lab. I am also grateful for the past lab members, Noah Robert, Anna Demarbre, and Heidi Nguyen, who were always a joy to talk to. Being surrounded by such thoughtful and supportive colleagues has made this experience both rewarding and meaningful. I am also grateful to have trained Kloe Mayhew, an undergraduate TMM student that I believe will do amazing in their future endeavours. Further, I would like to thank members of the Korneluk, Alain, MacKenzie, Pena, and Djaoud's laboratory members for the shared discourse around science and experiments.

To my family, thank you for your unconditional love, patience, and support throughout this journey. Your encouragement has carried me through the most challenging moments, and your belief in me has given me the confidence to keep moving forward. Each of you played such an important role in helping me reach this point. I am deeply grateful for the foundation you have given me, the values you have instilled in me, and the constant reminder that I am never doing any of this alone.

Finally, I would like to thank my friends, classmates, and the many student organizations I have had the privilege of being part of throughout my TMM/MSc journey. These communities shaped much of who I am today by giving me opportunities to lead, collaborate, mentor, and grow beyond the classroom and laboratory. The friendships, experiences, and lessons I gained through

these organizations have been invaluable, and I am grateful to everyone who supported and encouraged me throughout this chapter of my life.

LIST OF FIGURES

LIST OF TABLES

LIST OF TERMS & ABBREVIATIONS

APC	**Antigen-presenting cell**
B16F10-OVA	**Ovalbumin-expressing B16F10 melanoma cells**
BMDC	**Bone marrow-derived dendritic cell**
BSA	**Bovine serum albumin**
CCR7	**C-C chemokine receptor type 7**
CD3	**Cluster of differentiation 3**
CD4	**Cluster of differentiation 4**
CD8	**Cluster of differentiation 8**
CD11c	**Cluster of differentiation 11c**
CD25	**Cluster of differentiation 25**
CD40	**Cluster of differentiation 40**
CD69	**Cluster of differentiation 69**
CD80	**Cluster of differentiation 80**
CD86	**Cluster of differentiation 86**
CD107a	**Cluster of differentiation 107a**
cIAP1	**Cellular inhibitor of apoptosis protein 1**
cIAP2	**Cellular inhibitor of apoptosis protein 2**
CIC	**Cancer immunity cycle**
CTL	**Cytotoxic T lymphocyte**
DAMP	**Damage-associated molecular pattern**
DC	**Dendritic cell**
DMSO	**Dimethyl sulfoxide**
ECM	**Extracellular matrix**
E0771-OVA	**Ovalbumin-expressing E0771 cells**
ESCRT	**Endosomal sorting complex required for transport**
EV	**Extracellular vesicle**
FADD	**Fas-associated death domain protein**
FBS	**Fetal bovine serum**
GM-CSF	**Granulocyte-macrophage colony-stimulating factor**
H-2Kb	**Mouse major histocompatibility complex class I molecule**
H-2Kb-SIINFEKL	**MHCI-bound SIINFEKL complex**
HSP70	**Heat shock protein 70**

IAP	**Inhibitor of apoptosis protein**
IDO	**Idoleamine 2,3-dioxygenase**
IFNα	**Interferon alpha**
IFNβ	**Interferon beta**
IFNγ	**Interferon gamma**
IKK	**Inhibitor of NF-κB kinase**
IL-2	**Interleukin-2**
ILV	**Intraluminal vesicle**
JAWSII	**JAWSII dendritic cell line**
LCL161	**LCL161 SMAC mimetic**
LLC-OVA	**Ovalbumin-expressing Lewis lung carcinoma cells**
LPS	**Lipopolysaccharide**
MC38-OVA	**Ovalbumin-expressing MC38 colon carcinoma cells**
MHCI	**Major histocompatibility complex class I**
MHCII	**Major histocompatibility complex class II**
MISEV	**Minimal information for studies of extracellular vesicles**
MMP-9	**Matrix metalloproteinase-9**
MVB	**Multivesicular body**
NEMO	**NF-κB essential modulator**
NF-κB	**Nuclear factor kappa-light-chain-enhancer of activated B cells**
NIK	**NF-κB-inducing kinase**
NTA	**Nanoparticle tracking analysis**
OVA	**Ovalbumin**
OT-I	**Ovalbumin-specific $CD8^+$ T-cell receptor transgenic mouse model**
PBS	**Phosphate-buffered saline**
PD-L1	**Programmed cell death-ligand 1**
PD-1	**Programmed cell death protein 1**
PI	**Propidium iodide**
PRR	**Pattern recognition receptors**
PTEN	**Phosphatase and tensin homolog**
Rab27a/b	**Ras-related protein Rab27a/b**
RIPK1	**Receptor-interacting protein kinase 1**
sEV	**Small extracellular vesicle**
SIINFEKL	**OVA257–264 peptide**

SM	**SMAC mimetic**
SMC	**SMAC mimetic compound**
SMAC	**Second mitochondria-derived activator of caspases**
TCR	**T-cell receptor**
TLR	**Toll-like receptor**
TME	**Tumour microenvironment**
TNFα	**Tumour necrosis factor alpha**
TNFR1	**Tumour necrosis factor receptor 1**
TRAF2	**TNF receptor-associated factor 2**
TRAIL	**TNF-related apoptosis-inducing ligand**
TSG101	**Tumour susceptibility gene 101 protein**
VEGF	**Vascular endothelial growth factor**
XIAP	**X-linked inhibitor of apoptosis protein**

CHAPTER ONE: INTRODUCTION

1.1 Cancer: Overview

Cancer arises from a series of dysregulated intracellular and intercellular mechanisms, ultimately leading to tumour formation. Cancer can be broadly classified into solid tumours and hematologic cancers. Solid cancers form tumour masses, whereas blood cancers typically develop in the blood, bone marrow, or lymphatic system and often do not form solid tumours[1]. As one of the leading causes of death worldwide, cancer accounts for over 20 million new diagnoses each year[2]. In Canada alone, an estimated $7.5 billion is spent annually on cancer-associated expenses[3]. As such, this disease not only puts a socioemotional burden on the individuals and families experiencing it, but also an economic burden on healthcare facilities and treatment groups[4–6]. This multifaceted burden highlights the complexity of cancer as a disease, which is reflected in its diverse biological mechanisms. The hallmarks of cancer framework were originally introduced as six defining biological capabilities of cancer cells, but it has since been expanded to include additional hallmarks and enabling characteristics. More recent versions of the framework recognize approximately 12-14 cancer-associated features[7].

1.1.1 Tumour microenvironment

Over the past few decades, the area in which the tumour resides known as the tumour microenvironment (TME) has gained much more attention. The TME serves as a dynamic and highly interactive ecosystem that actively contributes to cancer development, progression, and treatment response[8]. The TME is composed of a heterogenous group of cells such as stromal cells (fibroblasts and pericytes) along with blood and lymphatic vasculature, making up the extracellular matrix (ECM), and with immune cells such as lymphocytes, macrophages, and other inflammatory cells. As the tumour cells continue to proliferate, they constantly remodel the surrounding

microenvironment through hypoxia, oxidative stress, acidosis, and abnormal stromal and immune signaling. Moreover, formation of abnormal blood and lymphatic vessels, necrotic regions, and reduced treatment efficiency will occur as the TME matures and progresses towards metastasis[8,9].

1.1.1.1 Barriers to treatment of cancer

Due to the complexity of cancer, resistance to certain therapies is often framed as a consequence of cancer cell intrinsic traits such as genetic instability or altered survival signaling; however, the most prominent barriers to effective treatment arise from the TME[8,10]. When therapeutic agents are used to treat cancer, abnormal vasculature in the TME reduces the convective flow and intratumoural distribution of these agents. Abnormalities in vasculature also create large diffusion distances and uneven oxygen delivery, creating hypoxic regions and heterogenous perfusion. Other than functionally impairing certain drug treatments, these hypoxic regions are strongly associated with poor responses to radiotherapy and chemotherapy[11]. Under these hypoxic conditions, tumour cells become resistant to apoptosis and demonstrate increased activation of resistance-associated pathways involving altered DNA damage responses, autophagy, and p53 signaling, further limiting drug access[12]. In parallel, impaired clearance of metabolic products contributes to acidosis, creating a low-pH environment that compromises pH dependent therapies[11]. The ECM also serves as a major barrier in treatment resistance. The ECM in the TME has increased deposition of stromal components such as collagen and hyaluronan, creating a dense, rigid, and pressurized architecture that lowers the bioavailability of drugs and immune effectors[13].

Additionally, the TME directly controls immune cell recruitment, localization, metabolism, and overall function. Effective anti-tumour immunity requires many effector T cells to infiltrate the tumour of interest. Thus, it can be understood that tumour exist as immune-inflamed (i.e. hot),

immune-excluded, or immune-desert states (i.e. cold)[14,15]. In immune-inflamed tumours, $CD8^+$ and $CD4^+$ T cells are present, however they are rendered dysfunctional by suppressive cells and inhibitory pathways. These include programmed death-ligand 1 (PD-L1), idoleamine 2,3-dioxygenase (IDO), regulatory T cells (Tregs), and anergy-associated programs that halt their effector capabilities in the region of interest[14,15]. In immune-excluded tumours, lymphocytes accumulate in the surrounding connective tissue due to dense collagen networks, abnormal vasculature, and stiffened matrix. These tumours often display high resistance to immune checkpoint (IC) therapies as the active immune cells are unable to reach the cancer cells[15,16]. In immune-desert tumours, insufficient dendritic cell (DC) maturation, immunologic tolerance, and defective priming prevent the generation of T cell responses[15].

Together, the TME contributes to the barriers of cancer treatments as it creates a highly protective niche around tumour cells through many factors that limit drug delivery, reduce treatment penetration, and promote adaptive resistance programs in malignant cells[11,17,18]. In addition to impairing therapeutic delivery, the TME is a key regulator of anti-tumour immunity, shaping whether immune cells can effectively recognize and eliminate tumour cells.

1.2 NF-κB pathway

Nuclear factor kappa B (NF-κB) is termed as a family of transcription factors that function as a central regulator of inflammatory signaling, immune response, cell survival, and cell fate decisions[19,20]. The mammalian NF-κB family is composed of five subunits: RelA (p65), RelB, c-Rel, NF-κB1 (p105/p50), and NF-κB2 (p100/p52). These subunits share a conserved Rel homology domain that mediates dimerization, DNA binding, and interaction with inhibitory IκB proteins[19,20]. RelA, RelB, and c-Rel contain transactivation domains and can directly promote

transcription, whereas p105 and p100 are synthesized as precursor proteins that undergo proteolytic processing to generate p50 and p52, respectively[19–22]. While in resting conditions, NF-κB dimers are retained in the cytoplasm with IκB members. After phosphorylation, ubiquitination, and degradation of IκB, the NF-κB complexes translocate into the nucleus and activate target genes[20].

Further, there are two principal routes in NF-κB signaling, the canonical and non-canonical pathways (**Figure 1**)[20,23]. The canonical pathway is activated via the pro-inflammatory cytokine TNFα or intracellularly via pathogenic stimuli or genotoxic stress that actives the IKK complex. The IKK complex is composed of IKKα, IKKβ, and NEMO. Activation of this complex results in phosphorylation and degradation of IκB and subsequent nuclear translocation of p50/RelA or related dimers[19,20,23]. The canonical pathway is dependent on signal relays involving TRAF proteins, TAK1, ubiquitin scaffolding, and receptor-proximal signaling complexes downstream of TNF receptors, and Toll-like receptors (TLRs)[23,24]. Contrastingly, the non-canonical pathway is activated via stabilization of NF-κB-inducing kinase (NIK), activation of IKKα homodimers, and phosphorylation-dependent processing of p100 to p52, thereby generating RelB/p52 dimers with distinct transcriptional outputs[19,20]. The non-canonical pathway is associated with signaling by selected TNF superfamily receptors, such as CD40 ligand, BAFF, and lymphotoxin-β receptors; implicating important functions in lymphoid organogenesis, T- and B-cell biology, and DC maturation[19,20,23].

The functional outcome of NF-κB signaling depends on the activating stimulus, the cellular and signaling context state, and the composition of the NF-κB dimer. Often, NF-κB promotes expression of anti-apoptotic and stress-adaptive genes that protect the cells from cytotoxic stimuli[25–27]. NF-κB can also participate in pro-apoptotic transcriptional programs under specific

cellular contexts. For example, NF-κB can regulate components of death receptor signaling, including TNF-related apoptosis-inducing ligand (TRAIL) receptors and Fas/FasL-associated pathways, and may also interact with p53-dependent stress responses to promote apoptosis[27].

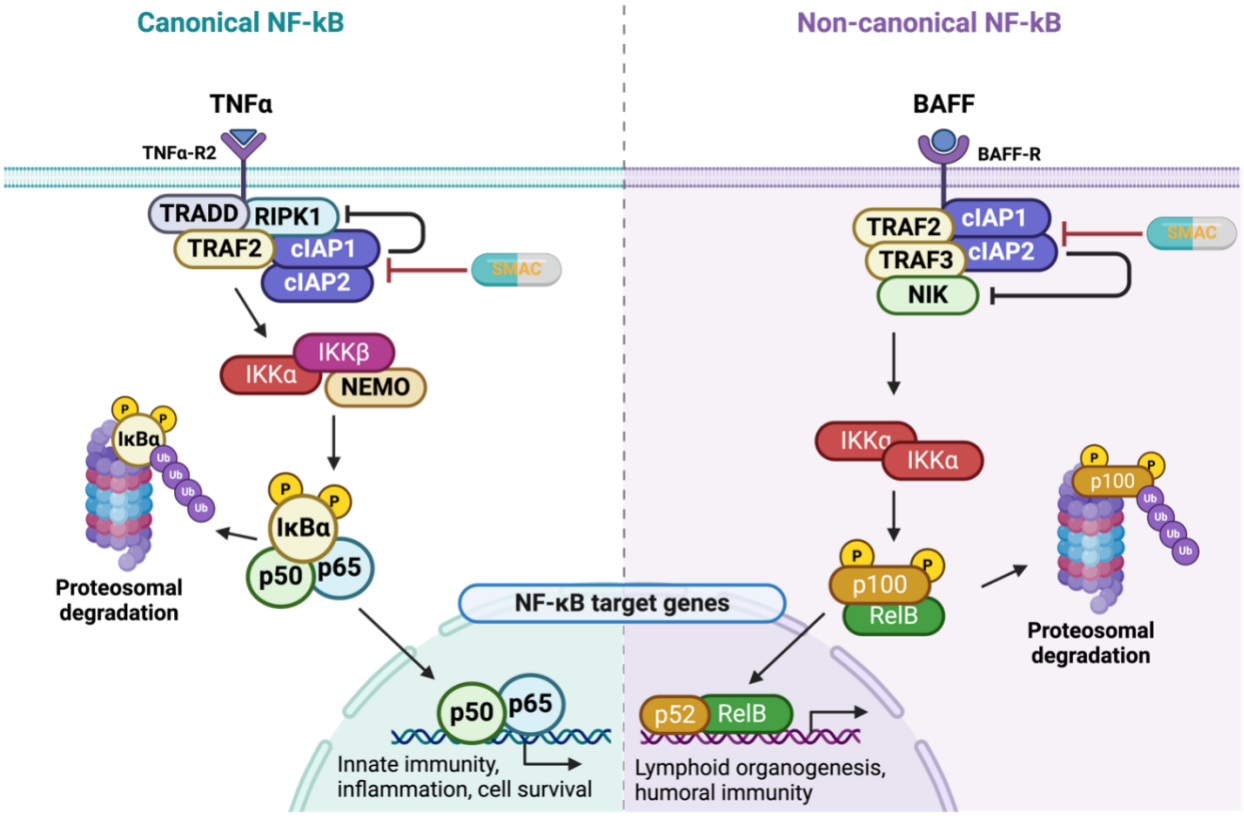

Figure 1. Canonical and non-canonical NF-κB signaling pathways and the role of cIAPs. The NF-κB pathway exists in two forms: the canonical (left) and non-canonical (right) pathways. In the canonical (classical) pathway, receptor activation leads to IKK complex-mediated phosphorylation of IκBα, triggering its ubiquitination and degradation, allowing NF-κB to regulate aspects of inflammation and cell survival. The non-canonical (alternative) pathway relies on NIK stabilization and IKKα-mediated p100 processing into p52 and RelB, promoting immune homeostasis. cIAP1/2 regulate both pathways by positively regulating the canonical NF-κB pathway through ubiquitination of RIPK1 as well by primarily suppressing the non-canonical NF-κB pathway by degrading NIK, a key kinase. SMs promotes the loss of the cIAPs, thereby shifting the NF-κB pathway to TNFα-mediated apoptosis and activation of the non-canonical NF-κB signaling pathway.

1.2.1 NF-κB in cancer

In the context of cancer, many malignancies are associated with abnormal and constitutive NF-κB activation[20,28]. In terms of the TME, NF-κB can be activated within stromal, immune, and tumour cells, allowing the pathway to shape tumourigenesis autonomously. In inflammatory microenvironments, cytokines such as TNFα, IL-1, and IL-6 activate NF-κB in pre-malignant or malignant cells. This will induce transcriptional programs that support factors such as proliferation, survival, angiogenesis, and metastatic dissemination[23,29,30]. To favour cancer progression in the TME, NF-κB signaling in recruited inflammatory cells can promote secretion of various cytokines, growth factors, and reactive oxygen species[23,31].

One of the major oncogenic consequences of NF-κB activation is enhanced tumour cell survival. The NF-κB pathway regulates many genes involved in cell-cycle progression, inhibition of apoptosis, cytokine production, and adhesion; thus, even under inflammatory and genotoxic stress, tumour cells continue to grow[20,31]. Moreover, NF-κB activation in tumours have a multitude of effects. In prostate cancer, phosphorylation of p65 promotes cell motility and oncogenic transformation[32]. While in colorectal cancer, IL-1β/NF-κB signaling has been shown to enhance proliferation through an miR-181a-dependent repression of the phosphatase and tensin homolog (PTEN)[33]. Further in breast cancer, constant NF-κB activation is associated with expression of pro-metastatic and pro-angiogenic targets such as vascular endothelial growth factor (VEGF) and matrix mateeloproteinase-9 (MMP-9)[34]. However, the effects of NF-κB varies from tumour type, diagnosis stage, and cellular compartment[23].

NF-κB is able to act as a key transcriptional mediator for the TNF-family receptor. TNF is able to activate protein-synthesis-independent cytotoxic mechanisms and protein-synthesis-dependent protective programs[20,25,26]. In human liver cancer cells, TRAIL induces NF-κB activation through

a TRAF2-NIK-IKK cascade, and inhibition of NF-κB exposes apoptotic signaling involving fas-associated death domain (FADD), caspase-8 and -3, and mitochondrial permeability transition[25], this serves as a critical anti-apoptotic checkpoint that aids malignant cells from death receptor-mediated cytotoxicity[35,36]. Further, NF-κB is also integrated with other stress-response pathways that influence treatment outcome. These affected outcomes include pathways related to p53, autophagy, and mitochondrial apoptosis signaling[27,34,37].

Overall, the NF-κB pathways are a central and highly-context dependent signaling pathway in cancer biology. In many tumours, persistent NF-κB activation supports factors such as proliferation, angiogenesis, inflammation, and therapeutic resistance, thereby reinforcing multiple hallmarks of cancer progression. It is also important to remark that the function of apoptosis is dependent on the activating stimulus, cellular background, and transcriptional context[7,20,23,29,31,36].

1.3 Inhibitors of apoptosis

The inhibitor of apoptosis (IAP) proteins are a family of anti-apoptotic regulators defined by the presence of at least one baculoviral IAP repeat (BIR) domain (**Figure 2**). The BIR domain is a zinc-binding protein-protein interaction module that plays an important role in their signaling activitiy[38]. In cancer, over-expression and dysregulation of the IAPs leads to manifestations such as resisting cell death, avoiding immune destruction, and contributing to metastasis, thus causing resistance to chemo- and radiation therapies[38–42]. The IAP family comprises eight members; among these, X-linked IAP (XIAP) and cellular IAP1 and 2 (cIAP1, cIAP2) are among the most well characterized[43]. XIAP, cIAP1, and cIAP2 have three BIR domains and a C-terminal RING domain; additionally, cIAP1 and cIAP2 contain a caspase recruitment domain (CARD) domain that contributes to E3 ligase activity[38,44]. The RING domain provides E3 ligase function, which allows

these IAPs to catalyze ubiquitylation reactions that influence the overall signaling properties of different substrates and themselves.

XIAP is best known for its ability to directly inhibit caspases, whereas cIAP1 and cIAP2 primarily regulate cell death and survival signaling through their E3 ubiquitin ligase activity[39,44]. XIAP is regarded as the strongest direct endogenous caspase inhibitor among the IAPs[40]. In terms of mechanism, the linker region preceding XIAP BIR2 inhibits caspase-3 and caspase-7, while the BIR3 domain binds caspase-9 and prevents its activation[40,44,45]. cIAP1 and cIAP2, however, control signaling complexes via their RING-dependent ubiquitin ligase acitiviy[46].

Moreover, the anti-apoptotic effects of cIAP1/2 are especially evident in TNF receptor-associated signaling complexes. cIAPs are recruited through a BIR1-mediated interaction with TRAF proteins[44,46]. cIAPs promote K63-linked ubiquitylation of RIP1, which favors the assembly of pro-survival signaling complexes and supports further activation of downstream survival pathways[46]. The degradation of cIAP1/2 leads to lack of RIP1 ubiquitylation; engagement of this pathway via TNFα renders cells to be more permissive to caspase-8 activation and apoptotic cell death[44,46].

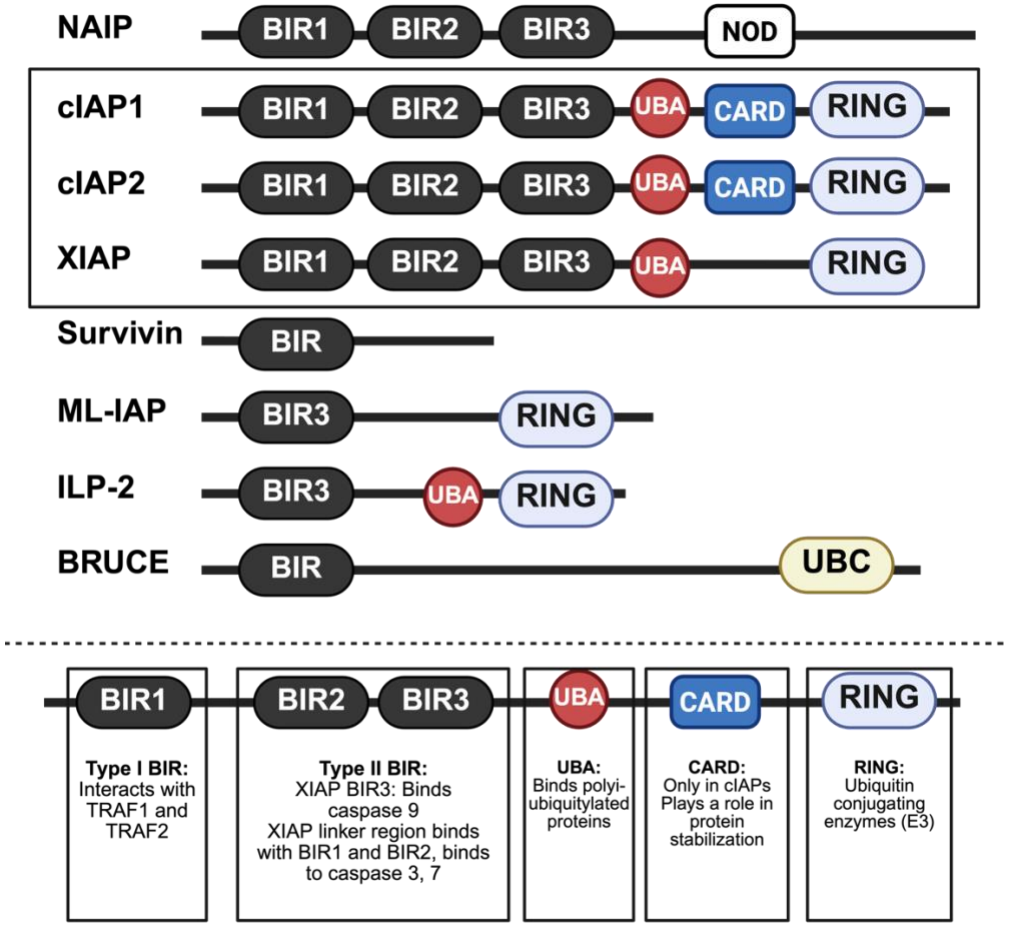

Figure 2. Structural differences among the inhibitor of apoptosis (IAP) family. Members of the IAP family are defined through the presence of one or more baculoviral IAP repeat (BIR) domains, which mediate interactions with caspases and other signaling proteins. Additional domains such as ubiquitin-associated (UBA), caspase recruitment (CARD), nucleotide-binding oligomerization (NOD), and RING domains, distinguish individual IAP members and contribute to their unique functionality.

1.3.1 IAP antagonism: SMAC mimetics

The Second mitochondrial-derived activator of caspases (SMAC/DIABLO) protein serves as an endogenous antagonist of that IAPs. SMAC is processed and released into the cytosol upon apoptotic stimulation[38,44]. Cytosolic SMAC harbours an N-terminal Ala-Val-Pro-Ile (AVPI) motif that binds XIAP, cIAP1, and cIAP2, which removes the IAP-mediated suppression of apoptosis[41,44,45]. SMAC competes for binding to the BIR domain on XIAP, leading to inability of XIAP to block caspase activity. As for cIAP1/2, SMAC binding promotes cIAP1/2 autoubiquitylation and proteasomal degradation, thus removing an upstream break on death signaling[45,47]. However, the IAPs also facilitate proteasomal degradation of SMAC/DIABLO through their E3 ubiquitin ligase function, thereby counteracting its apoptotic effects[44,48]. This then provides a rationale for having a made antagonist that is SMAC-like, to re-engage cell death pathways in tumour cells that have dysregulated IAPs.

Consequently, SMAC mimetic (SM) compounds have been developed. SMs are a small molecule peptide memetic of the endogenous protein SMAC/DIABLO. SMs induce the degradation of cIAP1, cIAP2, and XIAP, thereby sensitizing cancer cells TNFα-mediated apoptosis (**Figure 3**)[44,49]. Both monovalent and bivalent forms of SMs have been developed, as well as non-peptide versions designed to enhance therapeutic efficacy[50]. In terms of clinical efficacy, SMs are still under ongoing clinical trials. SMs such as LCL161, and Birinapant, are the most historically completed[51,52]. Currently, Tolinapant (ASTX660, **Table 1**) are in phase I/II clinical trials for a few different tumours[53].

At a molecular level, apoptosis is executed through a proteolytic cascade of caspases, in which initiation of caspases activation downstream effector caspases such as caspase-3, leading to cleavage of key cellular substrates[54,55]. This process is divided into two major pathways: intrinsic,

a mitochondria-mediated pathway, and extrinsic, a death receptor-mediated pathway[56]. The intrinsic pathway is activated by intracellular stress signals that promote mitochondrial outer membrane permeabilization, resulting in the release of cytochrome c into the cytosol[57]. Once released, cytochrome c works with dATP and Apaf-1 to form the apoptosome, which recruits and activates caspase-9 to initiate the downstream apoptotic protease cascade[58]. Further, the extrinsic pathway is initiated when death ligands engage death receptors, leading to recruitment of adaptor proteins such as the FADD and activation of caspase-8 within the death-inducing signaling complex[59]. Activated caspase-8 will directly activate executioner caspases through the cleavage of BID, which signals cytochrome c release[60,61]. Through the degradation of cIAP1/2, SMs shift TNF receptor signaling away from pro-survival signaling to caspase-8 activation, thereby engaging the extrinsic apoptotic pathway[62]. Additionally, by antagonizing XIAP, SMs allow the apoptotic cascade to proceed more efficiently when the initiation of the intrinsic or extrinsic pathway has started[63].

Over the past decade, SMs have been shown to display immunomodulatory effects by activating type I interferon signaling, macrophage activity, and enhancing cytokine release[64–67]. Furthermore, SMs, particularly LCL161, have shown greater efficacy when used in combination with other therapies, indicating that combination therapy or adjuvants may be essential for their clinical development[68–71]. These ongoing studies make SMs a promising anti-cancer and immune-enhancing therapy.

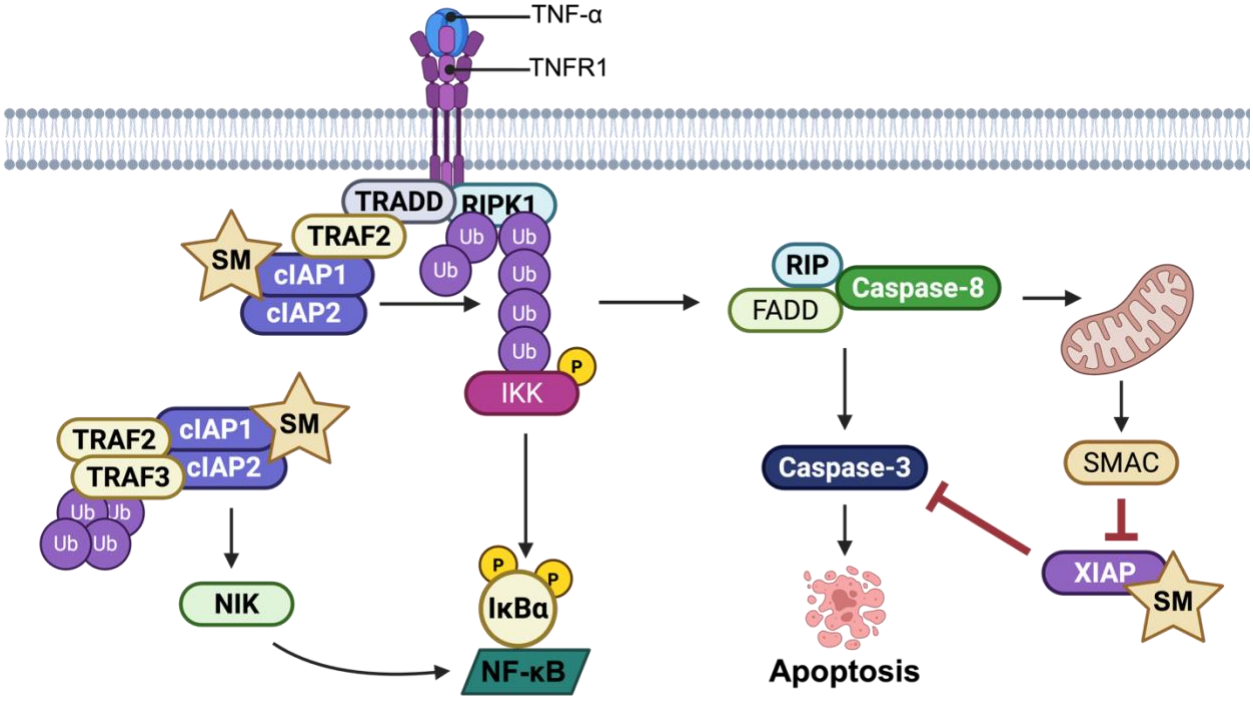

Figure 3. Inhibitor of Apoptosis (IAP) protein signaling with the placement and activity of SMAC mimetics as IAP antagonists. Following TNFα binding to TNF-R1, adaptor proteins including TRADD, RIPK1, TRAF2 and cIAPs are recruited to promote RIP ubiquitination and downstream IKK/NF-κB signaling. IAP antagonists, such as SMs target cIAPs and XIAP, disrupting pro-survival signaling and relieves XIAP-mediated inhibition of caspase-3.

Table 1. Current active clinical trials regarding compounds of SMAC mimetics

SMAC Mimetic	Current Trial Focus	Phase/Status
Tolinapant (ASTX660)	Lymphoma, Solid Tumours	Phase I/II, Active
ASTEROID: Tolinapant (ASTX660) with Pembrolizumab	Advanced Cancer, Cervical Cancer, Triple Negative Breast Cancer	Phase I, Active
Tolinapant (ASTX660)	Locally advanced Rectal Cancer	Phase I, Active
Birinapant and re-irradation therapy	Locoregionally recurrent head and neck squamous cell carcinoma	Phase I, Active
Tolinapant (ASTX660) and oral decitabine/cedazuridine	Relapsed/refractory peripheral T cell lymphoma	Phase I, Active

1.4 Immunity

In cancer, the immune system serves as an active determinant of tumour fate that can recognize and eliminate immunogenic tumour variants while also imposing selective pressure that drives tumour evolution towards immune escape[72,73]. This selective pressure is often recognized as immunoediting through three phases: elimination, equilibrium, and escape. In the elimination phase, immune cells such as cytotoxic T cells recognize and destroy emerging tumour cells. The equilibrium phase begins when tumour cells have been missed during the elimination phase. During this period, tumour cells may accumulate genetic and epigenetic changes that enhance their survival under immune pressure. Eventually, in the escape phase, resistant tumour variants proliferate unchecked as they develop mechanisms to evade immune detection or suppress immune responses leading to cancer[74–76]. Thus, effective anti-tumour immunity is a process involving continuous interactions between cancer cells, stromal elements, and immune populations both within and beyond the TME[72,77]. Further, tumour immunity is fundamentally systemic. Key priming events occur in lymphoid tissues, myeloid cells are continuously produced in the bone marrow, and anti-tumour responses are ongoing between the tumour and the periphery tissues[77,78]. As such, both innate and adaptive immunity contribute to the regulation of cancer; with the innate immune system shaping early inflammatory responses and the adaptive immune system providing antigen-specific cytotoxicity and immunological memory[73,79].

The innate immune system is the body's first line of defense. This immediate and nonspecific response is done by molecules such as pattern recognition receptors (PRR), such as TLRs, that detect pathogens and abnormal cells. Dendritic cells (DCs) are an important bridge between innate and adaptive immunity. In their immature state, DCs reside at sites of pathogen entry, capturing antigens through phagocytosis and other endocytic pathways while simultaneously

detecting danger signals through PRRs. Once activated, DCs undergo maturing that is characterized by enhanced antigen processing, stabilization of peptide-loaded major histocompatibility complex (MHC) molecules, upregulation of C-C chemokine receptor type 7 (CCR7), and increased expression of costimulatory molecules such as CD40, CD80, and CD86[80,81]. Through these changes, it enables their migration to draining lymph nodes, where mature DCs present their antigenic peptides to antigen-specific $CD8^+$ or $CD4^+$ T cells to initiate tumour-specific immunity[72,73,77,80,81]. $CD8^+$ cytotoxic T cells serve as critical adaptive effectors responsible for identifying and killing tumour cells. $CD8^+$ T cell's function depends on the recognition of antigenic peptides presented by MHCI complexes on target cells[17,73]. Upon activation of $CD8^+$ cytotoxic T cells, these cells mediate tumour cell killing through granule exocytosis, Fas Ligand (FasL)-mediated apoptosis, as well as production of cytokines such as IFNγ and TNFα[17]. $CD4^+$ T cells, also known as helper T cells, direct immune response against pathogens through the release of many cytokines such as IFNγ and IL-2. Further, $CD4^+$ T cells promote $CD8^+$ T cell priming through CD40/CD40L interactions and promote memory formation[17].

Despite the presence of protective immune mechanisms, oncogenesis, the process by which healthy cells transform into cancer cells can still occur. The complexity and consistent change of tumours allow them to impair recognition, remodel the immune landscape, and suppress effector functions[72,73]. One major mechanism of immune evasion is a loss or downregulation of MHCI mediated antigen presentation. Although this makes tumour cells more vulnerable to natural killer cells through the innate immune system, it results in the suppression of $CD8^+$ T cell mediated cytotoxicity as cell surface MHCI displays are weakened[82]. Moreover, DCs in the TME may be halted in an immature or tolerogenic state. Local immunosuppressive factors such as interleukin-10 (IL-10) and transforming growth factor-β (TGFβ) can shift antigen presenting cells towards

phenotypes that favour Treg expansion rather than effective T cell activation[14,72]. As a result, this tumour burden drives not only local immune processes within the TME but also reorganizes immune populations systemically.

Overall, the fate of anti-tumour immunity is determined by successful capture, presentation, and recognition of tumour-derived antigens within the evolving tumour microenvironment.

1.4.1 Tumour antigens

Tumour antigens (tAgs) are crucial for the adaptive immune system as it serves as the molecular basis for determining the difference between malignant and healthy cells. tAgs are characterized as a heterogenous group of targets that differ in origin, specificity, and therapeutic relevance. As explained, recognition of tumour antigen through MHCI complexes by $CD8^+$ cytotoxic T cells is a central step in immune-mediated tumour control[83]. There are three main types of tAgs, tumour-specific antigens (TSAs), tumour-associated antigens (TAAs), as well as cancer-germline antigens[84]. TSAs are exclusively found on tumour cells, while TAAs are present on both normal and tumour cells in different concentrations. Cancer-germline antigens, on the other hand, are expressed on germline cells in the testes or ovaries[84,85]. Professional antigen presenting cells, such as DCs, play a pivotal role in initiating an immune response. They capture tAgs through phagocytosis or endocytosis, process them into peptides, and present them on their MHC molecules to then activate specific T cell response. However, it is important to note that antigenicity alone is insufficient to guarantee immunity, as immunogenicity is dependent on how well the specific antigen can cause an immune response. Factors such as peptide stability, HLA binding, and T cell recognition contribute to this[83].

Preclinical studies commonly employ defined model antigens to understand and identify antigen processioning, presentation, and antigen-specific T cell responses under controlled conditions. Ovalbumin (OVA) serves as one such model antigen.

1.4.1.1 OVA as a model antigen

OVA is a protein derived from chicken albumin that has been widely adopted as a model antigen for antigen-specific immune response in both *in vitro* and *in vivo* studies[77,86]. Notably, OVA can be considered as a model antigen that mimics a tumour neoantigen[87]. Further, the sequence and immunogenic epitopes of OVA are well characterized, making the model a controlled system. This characteristic makes OVA useful in cancer immunology as it can provide specific and precise answers in the context of antigen processing, presentation and recognition of antigen, and overall functional anti-tumour responses[83,87]. Both MHC class I- and MHC class II-restricted immunity can be analyzed using OVA specific peptide epitopes and cognate transgenic T cell systems[86,88].

A common OVA-derived MHCI epitope is SIINFEKL, which corresponds to amino acids 257-264. OVA is presented on H-2K^{b} and elicits a strong CD8^{+} cytotoxic T cell response[86,88]. Suitably, OT-I T cells are designed to recognize SIINFEKL in the context of H-2K^{b} and have become a standard tool for evaluating antigen cross-presentation and CD8^{+} T cell activation. In parallel, OVA also contains MHCII relevant sequences. This includes peptide 323-339, which is used to study CD4^{+} T cell and B cell responses. With both OVA sequences, it provides an attractive method to examine multiple viewpoints of adaptive immune responses in an experimental system[86,88]. The OVA model has been incorporated into multiple tumour models such as B16-OVA melanoma and E.G7 lymphoma, allowing studies to assess how known antigens behaves in the

context of tumour growth, vaccine design, and tumour challenge[87,88]. Moreover, tumour cell lines engineered to express OVA have been proved useful for examining humoral immunity[89].

While the OVA system has many strengths, it is important to note that it is a good mechanistic model rather than a proper representation of the full complexity of endogenous tAgs[87]. It has been shown that the protein contains multiple epitopes of differing immunogenicity and typicity, as not every peptide is able to elicit a $CD8^+$ T cell response in the context of tumour control. For instance, when SIINFEKL is administered prophylactically before tumour inoculation, it is able to elicit a strong immunogenic response; however, when the tumours are already established, the therapy becomes weaker[87]. Thus, OVA model is a powerful tool for studying antigen presentation, cross-priming, and tAg-specific lymphocyte responses, while also providing a note that anti-tumour immunity depends more than just antigen identity[87,88]. Its broader value also lies in illustrating how tAgs play a role in the sequential steps of the cancer immunity cycle.

1.4.2 Cancer immunity cycle

The Cancer Immunity cycle (CI cycle) is a positive feedback mechanism in which the immune system leverages tAgs to combat and suppress tumour development. The CI cycle is comprised of seven major steps, each acting as a rate limit step for the next (**Figure 4**)[90,91]. TAgs, DCs and T cells, serve as key players in the cycle. TAgs are released by cancer cells and are internalized by DCs. Once processed, these DCs mature into APCs as they present the processed tAg on their MHC class I and class II molecules. These APCs will then travel to the lymphoid organs to prime and activate antigen specific T cells. Once activated, the T cells travel through the bloodstream, infiltrate the TME, and target cancer cells for destruction. This eradication releases additional tAgs into the TME, enabling subsequent rounds of the CI cycle to be initiated. Through this process, the immune system continually amplifies its response against the tumour[91,92].

Further, effective initiation of the CI cycle depends on more than just antigen availability and the immunogenic context in which antigens are released plays a major factor role[93]. Upon tumour cell death, opposing immune system outcomes may happen, known as being either immunogenic or tolerogenic. Depending on the outcome, this will influence whether DCs will acquire a danger-associated signal to mature and prime to specific T cells[93]. As explained, following antigen uptake, DCs must mature, migrate to the lymph node, and provide appropriate activation cues to naïve T cells[91,92,94,95]. Effective $CD8^+$ T cell priming is done through a three-signal model. Signal 1, wherein there is T cell receptor recognition of peptide-MHC complexes; Signal 2, interactions such as CD80/CD86 from APCs to CD28 on T cell provide costimulatory signals; and Signal 3, cytokines such as IL-12, type I interferons, and IL-2 in the microenvironment bind to cytokine receptors on the T cell[96]. Once completed, recognition of tumour cells then depends on productive interaction between the T cell receptor and peptide-loaded MHC molecules on the cancer cell themselves. Once detected, CD8 T cells mediate the tumour killing via perforin- and granzyme-dependent mechanisms[73,95].

It is also important to mention that each of these steps functions as a rate-limiting point, and disruptions at any stage can impair the generation of a strong anti-tumour response[95,97]. Immune activation and recognition may be poor due to certain tumours possessing low mutational burden or antigen loss. Additionally, DC dysfunction can prevent adequate antigen presentation and weaken downstream T cell priming[97]. Inhibitory pathways involving cytotoxic T-lymphocyte-associated protein 4 (CTLA-4) and PD-1 can attenuate activation and expansion of tumour-reactive T cells[93]. Further, effective target recognition may be lost through tumour-associated defects in antigen presentation machinery. This would include variations in HLA-associated pathways such as β2-microglobulin, or tapasin, reducing immune visibility[95,97]. Once in the TME, the presence of

Tregs, tumour-associated macrophages, myeloid derived suppressor cells, and chronic signalling environments will propel $CD8^+$ T cells into dysfunction and exhaustion[95,96].

Overall, the CI cycle not only provides a conceptual foundation for understanding how effective anti-tumour immune responses are generated but also highlights the specific biological barriers that may persist at every step. Thus, the concept of cancer immunotherapy is structured to exploit this barrier.

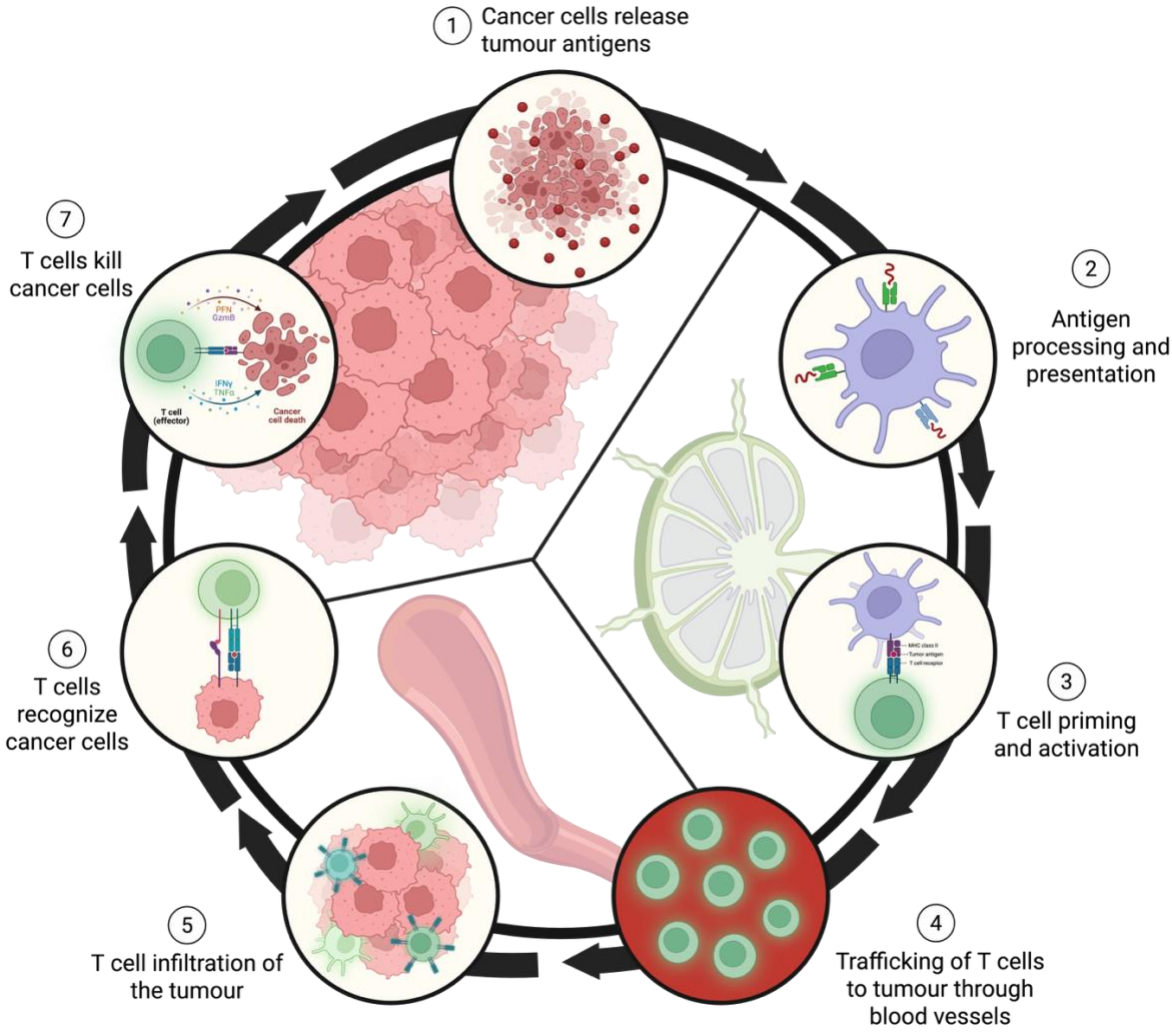

Figure 4. Overview of the cancer immunity cycle. Tumour cell death releases tumour-associated/specific antigens, which are captured and processed by antigen-presenting cells. These antigen-presenting cells then migrate to the lymph nodes, where they prime and activate tumour-specific T cells through antigen presentation and co-stimulatory signaling. Once activated, tumour-specific T cells will enter the circulation and infiltrate the tumour microenvironment and recognize the cancer cells displaying the tumour antigens on their MHC molecules. This will enable the cytotoxic T cell to eradicate tumours, resulting further antigen release and continued immune amplification.

1.4.3 Cancer Immunotherapy

Cancer immunotherapy is a form of cancer therapy that utilizes the body's immune system to identify and eliminate cancer cells. Current advancements include immune checkpoint inhibitors, adoptive therapies such as CAR-T cell therapy, the use of nanoparticles to remodel the TME, and oncolytic viruses[98–100]. Moreover, SMs have been proven to enhance the efficacy of immune checkpoint inhibitors, CAR-T cell therapies, and cancer vaccines by amplifying the anti-cancer immune response[66,68–71,101]. While there have been many advancements in cancer immunotherapy, a significant barrier would be the multifaceted mechanisms tumours may have or acquire. As said, tumours can perform tasks such as recruiting suppressive cells, alter antigen presentation machinery, as well as upregulating immune checkpoints[93,95,96]. There has been an increased understanding in the role immune cell-derived extracellular vesicles (EVs) in immunity. Immune cell-derived vesicles can facilitate the CI cycle by mediating the cross talk between innate and adaptive immunity[102].

1.5 Extracellular vesicles

EVs are classified as a heterogenous population of membrane-bound particles naturally released by a multitude of cells with a lipid bilayer. The category of EV is understood as an umbrella term that encompasses vesicles of different origins, sizes, and functions rather than one singular entity[103,104]. EVs are present in many biological fluids as they are virtually released by every cell type; thus, these EVs play a critical role in intercellular communication[105]. EVs commonly include exosomes (sEVs), microvesicles or ectosomes, apoptotic bodies, and other related particles. An important factor is whether they arise from the endosomal system or directly from the plasma membrane[104,106]. To classify subsets of sEVs, the minimal information for studies of extracellular vesicles (MISEV) guidelines are followed[107,108].

1.5.1 Small Extracellular Vesicles

sEVs are a subset of EVs measuring approximately 30-150 nm in diameter. sEVs have a critical role in intercellular communication due to their ability to carry and transfer bioactive cargo to recipient cells, thereby influencing cellular functions including within the TME. The biogenesis of sEVs may stem from two pathways: the endosomal sorting complex required for transport (ESCRT)-dependent or the ESCRT-independent pathway. The ESCRT-dependent pathway relies on a series of protein complexes, namely, ESCRT-0, I, II, and III, along with associated proteins such as VPS4 and TSG101. The ESCRT-dependent pathway generates sEVs through the invagination of the endosomal membrane to create intraluminal vesicles (ILVs). Numerous ILVs are then stored inside a specialized endosome called a multivesicular body (MVB). MVBs then fuse with the plasma membrane, releasing sEVs into the extracellular space. In contrast, the ESCRT-independent pathway does not use the protein complexes; rather this pathway relies on lipid molecules such as ceramides, sphingolipids, and cholesterol to aid in the formation of sEVs within MVBs[109,110]. Regardless of the pathway of origin, all sEVs can encapsulate bioactive cargo such as nucleic acids, proteins, and lipids. Importantly, sEVs are released by virtually every cell type including neoplastic cells[111–114].

Over the past decade, advancements in our understanding of sEVs have highlighted their therapeutic potential, particularly in the ability to deliver small interfering RNAs (siRNAs), microRNAs, and chemotherapeutics to specific target sites[111,115]. sEVs are commonly used as a diagnostic tool for a variety of diseases as they can be found in all biological fluids[114,116–118]. However, sEVs can also contribute to cancer progression by carrying growth-promoting factors, oncogenic miRNAs, and tAgs that drive cancer cell proliferation. Tumour-derived sEVs may also express molecules such as PD-L1, which inhibits activity of cytotoxic T cells[114,119]. In contrast,

DCs can release sEVs that mirror their antigen presenting capabilities, thus playing a critical role in immune modulation. Notably, these DC-derived sEVs carry tumour antigens and MHCI and II molecules on the surface, allowing them to prime and activate cytotoxic T cells[90,113,120,115,121,91]. Overall, due to their diverse functions and significant therapeutic potential, there is a growing interest in extracellular vesicles, particularly sEVs, as promising tools not only for diagnostic applications but also as carriers for biomolecules and drugs.

1.5.2 EVs in an immunity context

sEVs have been described as mediators of disease progression that can suppress or impair immune responses[122,123]. Conversely, sEVs can also transfer antigens from their cell of origin to APCs for uptake and processing[124]. The role of sEVs in the TME is especially important, as they govern how tumour cells communicate with stromal and immune populations, thereby influencing whether anti-tumour immunity is suppressed or promoted. Within the TME, sEVs mediate both paracrine and autocrine communication and contribute to tumour development, and phenotypic changes in neighboring normal cells[9]. Antigen presentation by professional APCs, including DCs and macrophages, are essential for initiative of adaptive immunity. Therefore, the generation of antigen-bearing sEVs creates opportunities to manipulate immune activation through sEV-mediated intercellular communication.

The transfer and uptake of antigens through sEVs have been well documented. In cancer, tumour cells often increase sEV secretion, which may contribute to immune surveillance during early tumourigenesis[125–127]. These vesicles can carry TAAs that are taken up and processed by DCs, ultimately supporting T cell priming[128,129]. In addition to antigen transfer, sEVs can also remodel the TME through the delivery of immune-modulatory molecules. For example, activated helper T cell-derived sEVs can deliver IFNγ to macrophages, enhancing STING activation and

disrupting immunosuppressive features of the TME[130]. Further, given their ability to carry antigenic and immune-modulating cargo, sEVs are increasingly being investigated as a potential vaccine platform to enhance anti-tumour immunity.

1.6 Rationale and Hypothesis

There have been many advancements in cancer immunotherapy; however, critical gaps remain in our understanding of how to overcome immune resistance and effectively reshape the TME. SMs serve a promising class of immunomodulatory anti-cancer drugs that induce cancer cell death and increase the activity of many immune cells. Since SMs are currently being evaluated in multiple clinical trials in combination with other therapies, understanding the extent of these mimetics will aid in the development of more effective therapies. sEVs, as a natural carrier of bioactive cargo, offer a unique opportunity for not only disease diagnosis, but also to enhance immune modulation within the TME. Previous work from our group has shown that SM treatment can trigger EV release from APCs such as macrophages, suggesting that these agents may influence immune responses not only through direct effects on cells, but also through EV-mediated intercellular communication. This concept is further supported by existing literature demonstrating that EVs can influence multiple stages of the CI cycle, including antigen transfer, antigen-presenting cell activation, and downstream T cell priming[102]. Together, these findings suggest that SMs may enhance anti-tumour immunity not only by directly modulating immune cell activity, but also by promoting sEV-mediated antigen transfer, providing a strong rationale for investigating SM-induced sEVs as regulators of the CI cycle.

CHAPTER TWO: MATERIALS AND METHODS

2.1 Reagents, Antibodies, and Cell Culture Media

All reagents were purchased from the manufactures listed below and prepared according to the manufacturer's instructions unless otherwise stated. Working concentrations were prepared fresh in the appropriate complete culture medium immediately prior to use unless otherwise specified.

Puromycin dihydrochloride was obtained from Gold Biotechnology (P-600-100), and used for maintenance of antibiotic-selected cell lines at the final concentration of 2 μg/mL. Dimethyl sulfoxide (DMSO; Sigma-Aldrich, D1435-500ML) was used as the vehicle for LCL161 and was included as a vehicle control at an equivalent final concentration of % DMSO in all relevant experiments.

The SM LCL161 was obtained from Novartis and SelleckChem. LCL161 was dissolved in DMSO to generate a stock concentration of 10 mM, aliquoted and stored at -20ºC. For experimental treatments, LCL161 was diluted in complete culture medium in varying concentrations. Lipopolysaccharide (LPS) was obtained from InvivoGen, LPS-EK Ultrapure (tlrl-peklps) and used as a positive control for dendritic cell activation at a final concentration of 1 ng/mL.

Recombinant cytokines, including interferon β (IFNβ), tumour necrosis factor alpha (TNFα), and interferon γ (IFNγ), were obtained from R&D Systems (12400-1) and Life Technologies (300-01A-50UG, 315-05-100UG), respectively. Cytokines were reconstituted in appropriate manufacturer's instructions and stored at -80ºC. For treatments, cytokines were diluted in complete culture medium to final concentrations of: IFNβ (50 U/mL), TNFα (1 ng/mL), and IFNγ (250 U/mL).

Recombinant murine granulocyte-macrophage colony-stimulating factor (rmGM-CSF) was obtained from Life Technologies (315-03-50UG) and used for the differentiation and maintenance

of both JAWSII murine DCs and bone marrow-derived DCs (BMDCs) at a final concentration of 5 ng/mL and 20 ng/mL, respectively. The ovalbumin-derived peptide OVA257-264 (SIINFEKL), was obtained from InvivoGen (vac-sin) and used as a model antigen for MHC class I antigen presentation assays. SIINFEKL peptide was reconstituted in double distilled water and used at a final concentration of 1 mg/mL. Recombinant human interleukin-2 (IL-2) was obtained from R&D Systems (BT-002-AFL-01M/LQ) and used to support T cell culture and/or dendritic cell-T cell co-culture assays at a final concentration of 400 U/mL.

Antibodies used for flow cytometry and western blotting are listed in **Table 2**. Flow cytometry antibodies were diluted in FACS buffer containing 1X PBS, 1% BSA, and 0.05% sodium azide according to the manufacture's recommended dilution. Western blot antibodies were diluted in EveryBlot Blocking Buffer (12010020) from BioRad and used at the dilutions indicated in **Table 2.**

Table 2. List of Antibodies Used for Flow Cytometry and Western Blotting

Antibody	Product ID	Concentration	Respective Panel
CD11c – APC	Biolegend, 117310	0.25 ug/100uL	JAWSII/BMDC/OT-I T cell
CD11a – PECy7	Biolegend, 153107	0.2 ug/100uL	OT-I T cell
CD86 – PerCP	Biolegend, 105025	0.25 ug/100uL	JAWSII/BMDCs
CD40 – FITC	Biolegend, 102905	1 ug/100uL	JAWSII/BMDCs
CDC80 – BV711	Biolegend, 117310	0.5 ug/100uL	JAWSII/BMDCs
MHCII – BV605	Biolegend, 107639	0.4 ug/100uL	JAWSII/BMDCs
CD11b – APC/Cy.7	Biolegend, 101225	0.25 ug/100uL	JAWSII/BMDCs
MHCI-SIINFEKL – PE	Invitrogen, 12-5743-82	0.5 ug/100uL	JAWSII/BMDCs
CD8a – AF700	Biolegend, 100730	0.5 ug/100uL	OT-I T Cells
CD69 – BV650	Biolegend, 104541	0.5 ug/100uL	OT-I T Cells
PD-1 – APC/Fire 750	Biolegend, 135239	0.5 ug/100uL	OT-I T Cells
CD3 – BV785	Biolegend, 100232	0.5 ug/100uL	OT-I T Cells
Zombie Violet	Biolegend, 423114	0.2 ug/100uL	JAWSII/BMDC/OT-I T cell
Calnexin	Novus, NB100-1965	1:1000	Western Blotting Antibody
TSG101	Abcam, ab83	1:1000	Western Blotting Antibody
Syntenin-1	Novus, NBP1-33661	1:1000	Western Blotting Antibody

2.2 Cell Culture and Maintenance

All cell lines were obtained from ATCC and are registered at CHEO RI. Cells were cultured and maintained at 37ºC and 5% CO2. The cancer cells (B16F10-OVA, MC38-OVA, and LLC-OVA) expressing model antigen, OVA, was cultured in cell culture-treated 15 cm^3 dishes (Corning, 430599) in HyClone Dulbecco's Modified Eagle Medium (DMEM) (Cytiva, SH30022.01) supplemented with 10% heat inactivated fetal bovine serum (HI FBS) (Sigma-Aldrich, 22G107), 1% penicillin-streptomycin (Fisher Scientific, SV30010), and 2 mg/mL of puromycin. The E0771-OVA cancer cell line was cultured in cell culture-treated 15 cm^3 dishes in HyClone RPMI 1640 media (Cytiva, SH30027.01) supplemented with 10% HI FBS, 2.5 mM HEPES (Cytiva, SH30237.01), and 1% penicillin-streptomycin. Moreover, JAWSII murine DC cell line was cultured with RPMI 1640 medium supplemented with 10% HI FBS, 1% penicillin-streptomycin, and 5 ng/mL of rmGM-CSF. BMDCs were cultured with the same medium and supplements of JAWSII; however, 20 ng/mL of rmGM-CSF was used instead. OT-I T cells were cultured in RPMI 1640 medium with 10% HI FBS, 1% penicillin-streptomycin, and 200 U/mL of IL-2.

2.3 Primary Cell Isolation and Differentiation

For BMDCs, C57BL/6 mice obtained from The Jackson Laboratory were euthanized in a CO2 chamber in compliance with animal care guidelines. Femurs and tibias of the mice were removed and placed in a small Eppendorf tube with a hole at the bottom punctured with an 18-gauge needle. This tube was placed over a 1.5 mL Eppendorf tube. Tubes were placed over ice during transportation. Following, tubes were centrifuged at 10,000 x g for 5 minutes at 4ºC. The bone marrow suspension was then washed with RPMI 1640 media and centrifuged for 300 x g for 5 minutes at 4ºC. Resuspension of washed cells were cultured with complete RPMI media in 15 cm3

plate and supplemented with 20 ng/mL of rmGM-CSF. On Days 2 and 4, suspension cells were removed along with media and replaced with complete RPMI media and 20 ng/mL of rmGM-CSF. On Day 6, both non-adherent and semi-adherent cells were ready to be collected for experiments.

For OT-I T cell isolation, C57NL/6-Tg(TcraTcrb)1100Mjb/J transgenic mice from the Jackson Laboratory were used. Spleens and lymph nodes were isolated into gentleMACS C tubes from Miltenyi (130-093-237) and homogenized with the gentleMACS Octo Dissociator from Miltenyi (130-096-427) using the mouse spleen protocol. After mechanical dissociation, the cell suspension was passed through a 70 µm cell strainer from Fisher Scientific (22-363-548). Further, the cells were centrifuged in an Eppendorf centrifuge 5810R at 500 x g for 5 minutes at 4°C. After, these cells were resuspended in ACK lysis buffer (formulation: 150 mM NH4Cl, 10 mM KHCO3, 0.1 mM EDTA in H_2O) and incubated on ice for 5 minutes. Following incubation, 1X cold PBS from Fisher Scientific (BP661-50) was used and centrifuged at 500 x g for 5 minutes at 4°C. The mouse $CD8a^+$ T cell Isolation Kit from Miltenyi (130-095-236) was used to isolate $CD8^+$ T cells from splenocytes and lymphocytes following manufacturer's instructions.

2.4 Cell Viability Assays

B16F10-OVA, MC38-OVA, LLC-OVA, E0771-OVA, JAWSII, and BMDCs were seeded in a 96-well plate at a density of 5,000-15,000 cells per well in 100 uL of complete culture medium. Cells were incubated overnight at 37°C with 5% CO2 to allow them to adhere to the plate. The next day, cells were treated with LCL161, TNFα, IFNγ or a combination at the indicated concentrations in **Table 1**. Vehicle-treated cells were included as controls, with DMSO. Cells were incubated under standard culture conditions for 24, 48, and 72 hours.

Following treatment, Alamar blue (Resazurin sodium salt) from Sigma-Aldrich (62758-13-8) reagent was added directly to each well at a ratio of 1:7 (resazurin:media) and incubated for 1, 2 and 3 hours (until visible colour change) at 37°C and 5% CO_2. Signal was measured using the Synergy HTX plate reader on the Biotek Gen5 software and detecting a fluorescence of 530/590 nm.

Cell viability was normalized to the appropriate untreated control group, which was set to 100% viability. Data were reported as the raw signal intensity. Each condition was performed with three technical replicates per experiment.

2.5 Preparation of EV-Depleted Media

Extracellular vesicle-depleted fetal bovine serum (EV-depleted FBS) was prepared by ultracentrifugation. HI FBS was transferred into ultracentrifuge tubes and centrifuged at 100,000 x g for 10 hours at 4°C to pellet bovine serum-derived extracellular vesicles. Following centrifugation, the supernatant was collected without disturbing the pellet and transferred into a sterile conical tube. Collected supernatant was stored at -20°C until use. Repeated freeze-thaw cycles were avoided. EV-depleted culture medium was prepared by supplementing DMEM or RPMI 1640 with 10% EV-depleted FBS, with 1% penicillin-streptomycin, and any additional cell line-specific supplements.

2.6 sEV Isolation

Small extracellular vesicles (sEVs) were isolated from conditioned culture medium by differential centrifugation and ultracentrifugation. Cancer cell lines were seeded in 15 cm3 plates and cultured until approximately 70-80% confluent. Cells were then washed with 0.1X PBS from

Sigma Millipore (D8537) to remove residual serum-derived vesicles and cultured in complete medium containing EV-depleted FBS for 24-36 hours. Following the replenishing of EV-depleted complete medium, cells were treated with LCL161, IFNγ, TNFα, vehicle, or a combination.

Conditioned medium was collected and subjected to sequential centrifugation steps to remove cells, debris, and large vesicles. The medium was centrifuged at 500 x g for 5 minutes at 4°C to remove cells. The supernatant was then transferred to a new tube and centrifuged at 2,000 x g for 20 minutes to remove dead cells and large debris, followed by centrifugation at 12,000 x g for 35 minutes to remove larger extracellular vesicles and remaining debris.

The cleared conditioned medium was transferred to ultracentrifuge tubes from Beckman Coulter (344061) and centrifuged at 120,000 x g for 120 minutes at 4°C to pellet sEVs. Additionally, the sEV pellet was then washed with sterile 0.1X PBS and ultracentrifuged again at 120,000 x g for 120 minutes at 4°C. Following the wash, the final sEV pellet was resuspended in 200 uL of sterile 0.1X PBS.

2.6.1 sEV Storage

Isolated sEVs were immediately stored at -80°C in small aliquots until further analysis and experiments. Freeze-thaw cycles were minimized. Samples were kept in -80°C for no more than six months.

2.7 sEV Quantification and Characterization

Isolated sEVs were quantified and characterized using nanoparticle tracking analysis (NTA)[131], transmission electron microscopy (TEM), protein quantification, and western blot analysis. These methods were used to determine sEV size, morphology, protein content, and sEV markers.

Minimal information for studies of extracellular vesicles (MISEV 2018, 2023) guideline were followed[107,132].

2.7.1 Nanoparticle Tracking Analysis

Particle concentration and size distribution of isolated sEVs were measured by NTA using ZetaView Multiple Particle Tracker Analyzer (Malvern Particle Metrix). 102 nm polystyrene beads from Malvern (NC1148977) was used for size calibration of the instrument. sEV samples were diluted in sterile 0.1X PBS to achieve a particle concentration within the optimal detection range of the instrument. Dilutions were prepared at 1:1,000 to 1:10,000, concentration varied depending on the condition of treatment for sEVs. Five technical replicates were recorded using consistent acquisition settings.

2.7.2 Transmission Electron Microscopy

To assess the morphology of the isolated sEVs, TEM was used. 5-10 uL of purified sEVs were placed onto carbon-coated copper grids and incubated for 10 minutes to allow vesicle adsorption. Excess liquid was removed using a filter paper, and grids were washed with distilled water. Samples were negatively stained with uranyl acetate for 5 minutes, after which excess stain was removed, and grids were allowed to air dry. Grids were imaged using a JEOL JEM-1400Flash at 120 kV. TEM was performed by the TEM Core at the University of Ottawa.

2.8 Protein Quantification Assay

To assess for protein concentration of sEV preparations and cellular lysates, they were measured using a DC protein assay according to manufacturer's instructions. Protein standards

were prepared using bovine serum albumin (BSA) over a concentration range of 0 to 1.5 mg/mL. Samples were diluted in RIPA SDS lysis buffer as needed to fall within the range of the curve.

Standards and samples were added to a 96-well plate in triplicate, followed by addition of the working reagent. The plate was incubated for 15 minutes at room temperature, and absorbance was measured using a Synergy HTX plate reader on the Biotek Gen5 software. Further, protein concentration were calculated from the standard curve. This was then used to normalize samples for western blotting and downstream assays.

2.8.1 Western Blot Analysis of EV Makers

To assess the sEV markers, western blot analysis were performed. Isolated sEV samples and corresponding whole-cell lysates were lysed in RIPA buffer supplemented with protease/phosphatase inhibitors from Sigma (PPC1010). Protein concentration was determined using DC protein assay, and 10 ug of protein was prepared.

Samples were mixed with 4x Laemmli buffer from Bio-Rad (#1610747) and DTT, then heated at 100^{o}C for 5 minutes. Proteins were separated on a 10% SDS-PAGE gel and transferred onto nitrocellulose membranes. Membranes were blocked in EveryBlot Blocking Buffer from Bio-Rad (#12010020) for 5 minutes at room temperature.

Primary antibodies were applied against EV-associated markers (see **Table 2**), and the negative marker Calnexin was included. Following the washing step, membranes were incubated with fluorescent secondary antibodies for 1 hour at room temperature. Finally, protein bands were visualized using fluorescence imaging on the ODESSEY CLx imaging system.

2.9 sEV Uptake Assays

DCs, including JAWSII cells or BMDCs were seeded at 1.0 x 10^6 cells per well in 6 wells and incubated with B16F10-OVA derived sEVs at 10 µg/mL at 37°C and 5% CO_2. These sEVs were treated with a variety of combinations with SMs and cytokines. After one hour, the corresponding wells were treated with vehicle, 1 µg/mL of LPS or 1.0 µM SM for additional 23 hours. Control conditions were also included: untreated cells, and 1 µg/mL LPS and 10 µg/mL OVA peptide cells. sEV uptake was assessed by flow cytometry using the Cytek Northern Lights.

2.10 DC-T cell Co-Culture Assays

DCs, including JAWSII cells or BMDCs were seeded at 2.0 x 10^5 cells per well in 6 wells and incubated with B16F10-OVA derived sEVs at 10 µg/mL at 37°C and 5% CO_2. These sEVs were also treated with a variety of combinations with SMs and cytokines. After one hour, they were treated with vehicle, 1 µg/mL of LPS or 1.0 µM SM. After a 24 hour incubation, OT-I T cells were introduced at a 1:5 ratio (DCs to T cells), 1.0 x 10^6 T cells per well. The co-culture was supplemented with 400 U/mL of rh-IL-2 and incubated for 96 hours, additional treatment-free complete media was added. Following incubation, cells were collected and activation of OT-I cells were assessed by flow cytometry.

2.11 Flow Cytometry

JAWSII cells and BMDCs were washed with 0.1X PBS and stained for cell surface makers. Fc blocking and zombie violet (viability) dyes were stained at a ratio of 1:300 and 1:400, respectively. The antibodies included markers for CD11c, MHCII, CD80, CD86, CD40, CD11b, and MHCI-SIINFEKL.

As for T cell activation, along with Fc block and viability, markers such as CD11c, CD11b, CD69, CD8a, CD3, and PD-1 were included. Further, controls such as untreated, unstained, heat killed, and positive control was accounted for. Samples were read on the Northern Lights flow cytometer from Cytek.

2.12 Statistical Analysis

Statistical analyses were performed using GraphPad Prism version 11.0. Data for NTA and viability assays are presented as +/- SD. Flow cytometry data is presented as the number of events compared to percentage of the maximum.

CHAPTER THREE: RESULTS

3.1 Aim 1: Characterize sEVs from SM- and cytokine-treated cancer cells

SM and cytokine combination treatment displayed cancer cell-line specific effects on viability

To determine whether SM treatment and/or inflammatory cytokines alter sEV production, it is important to understand the sensitivity each cancer cell line has against said treatments. In this experiment, B16F10-OVA, LLC, E0771, and MC38-OVA cancer cells were treated with LCL161 alone or in combination with IFNγ or TNFα. Cell viability was monitored over a 72 hour period and the control was an untreated group (**Figure 5**).

In B16F10-OVA cells, treatment with the LCL161 alone did not significantly affect cell viability (**Figure 5A)**. B16F10-OVA cells are classified as highly aggressive, murine melanoma cells. Similarly, TNFα alone had minimal effects; presenting strong resistance to mono-treated drug and cytokine compounds. IFNγ was seen to cause a reduction of viability more noticeably at later time points. This effect was further seen in the combination treatment of LCL161 and IFNγ, where viability was reduced to approximately 60% by 48 hours. Conversely, the cells treated with the combination of LCL161 and TNFα displayed similar resistance to the single treatments.

MC38-OVA cancer cells displayed a singular difference in response (**Figure 5B)**. MC38-OVA is a murine colon adenocarcinoma cell line. LCL161 and IFNγ monotherapy had negligible impact on cell viability. However, MC38-OVA was transiently sensitive to TNFα monotherapy with viability rebounding at the 48 hour mark. As for combination treatments, LCL161 and IFNγ displayed no apparent difference, while the combination of LCL161 and TNFα lead to a synergistic cytotoxic effect.

E0771 cells were the most sensitive to the SM treatment among all cancer cells tested (**Figure 5C)**. E0771 is a medullary breast adenocarcinoma murine model. The viability of E0771 cells decreased drastically following LCL161 monotherapy, reaching a complete loss of viability by 24

hours. This was also evident in the combination treatments of LCL161 with IFNγ and TNFα. Contrastingly, cytokine-only conditions had limited effects. TNFα treated conditions displayed little to no decrease in viability, and IFNγ only treatment produced a partial decrease.

In addition, LLC cells showed a singular difference in response (**Figure 5D**). LLC is a murine lewis lung carcinoma cell line. LCL161 treatment alone produced little to no reduction in viability, and both IFNγ and TNFα mono-treatments caused only moderate decreases over time. The combination of LCL161 and IFNγ produced little to no reduction in viability. In contrast, the combination of LCL161 and TNFα resulted in complete loss of LLC cell viability.

E0771 cancer cells exhibit pronounced sensitivity to SM monotherapy

To further characterize the sensitivity of E0771 cells to SM treatment, cells were treated with varying concentrations of LCL161 ranging from 0 μM to 2.5μM and viability was then assessed over 72 hours. The rationale behind this was to determine whether cytotoxicity was restricted to higher concentrations or whether lower doses were sufficient to impair overall cell survival. E0771 cells demonstrated a pronounced sensitivity to LCL161 even at the lowest concentration tested (**Figure 6**).

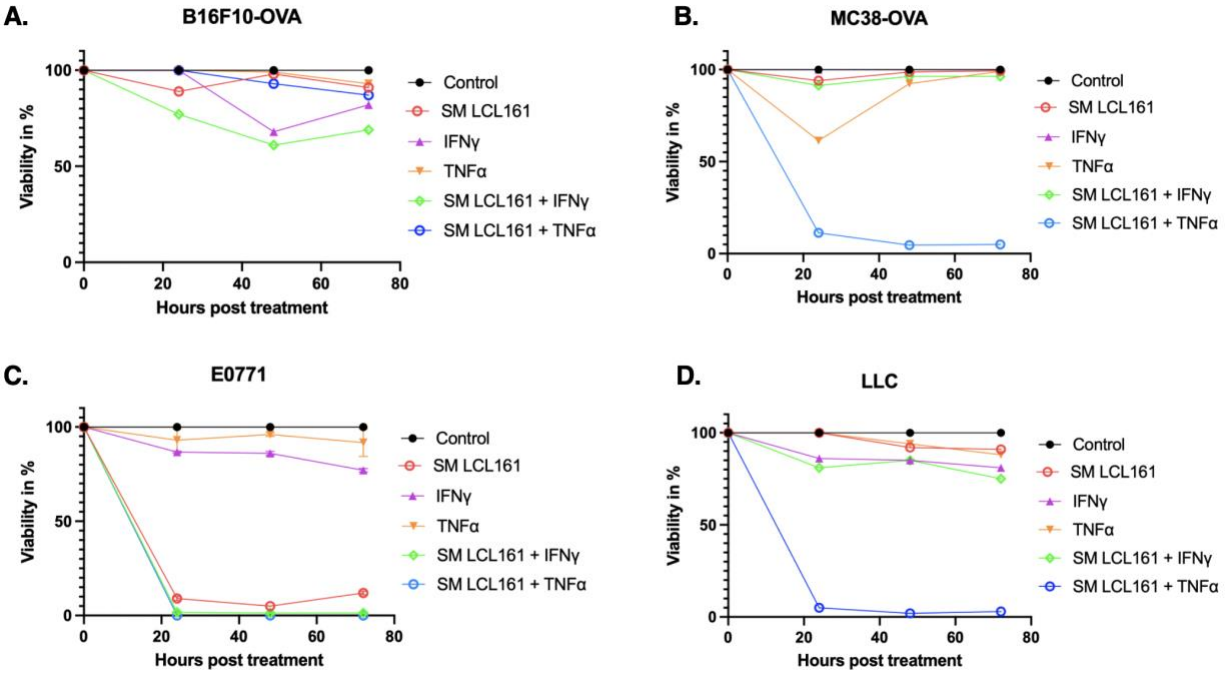

Figure 5. LCL161 and combination treatments alter viability in different cancer cell lines. Cancer cells (B16F10-OVA, MC38-OVA, E0771, and LLC) were treated with LCL161 and combination treatments at a concentration of 5μM and viability was assessed using Alamar blue assay at 24, 48, and 72 hours. Combination treatments include 250 U/mL of IFNγ, 1 ng/mL of TNFα, and DMSO as vehicle control. Error bars denote standard deviation (n=3 independent experiments with n=4 technical replicates, E0771. n=1, B16F10-OVA, MC38-OVA, LLC).

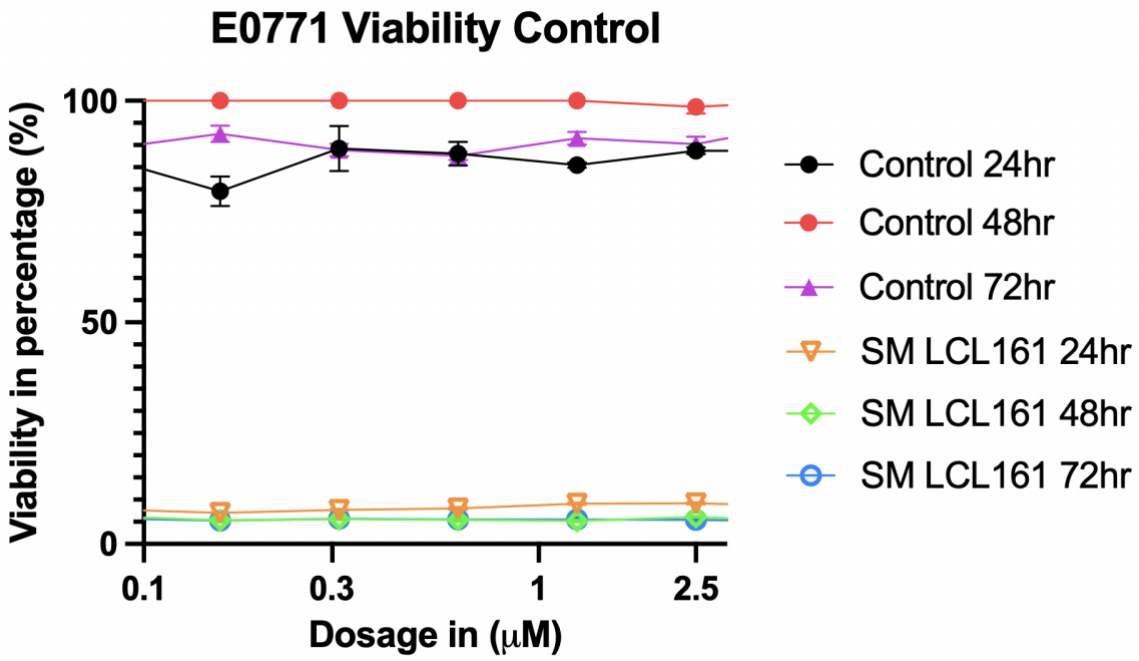

Figure 6. LCL161 kills E0771 murine medullary breast adenocarcinoma model at low concentrations. E0771 cells were treated with varying doses of LCL161 ranging from 0 μM to 2.5 μM. Viability was assessed using Alamar blue assay at 24, 48, and 72 hours post treatment. Error bars denote standard deviation (n=3).

SM and cytokine co-treatment increase EV release in SM refractory cancer cells

To determine whether SM alters EV production from cancer cells, conditioned media from SM-treated B16F10-OVA, MC38-OVA, and E0771-OVA cultures were collected. These conditions include vehicle (baseline control), LPS as a positive control, and LCL161. EV-enriched preparations were then analyzed by NTA to quantitate particle concentration and assess size distribution (**Figure 7**).

In B16F10-OVA cells, SM treatment significantly increased the quantity of particle release by a factor of ~21.7 compared to vehicle treatment and a factor of ~9.4 for LPS treated controls (**Figure 8A**). A similar trend was also observed in MC38-OVA cells whereby both LPS and LCL161 treatment was able to increase particle concentration relative to control conditions (**Figure 8B**). Treated MC38-OVA cells displayed an increased particle release factor of ~121.6 was seen in vehicle treatments compared to LCL161, and a factor of ~1.4 was seen in LPS treatments compared to LCL161. These findings demonstrate that SM-induced sEV release is not restricted to a single cancer cell line. Contrastingly, LCL161 does not increase the release of sEVs in E0771-OVA cancer cells (**Figure 8E**).

The role of inflammatory cytokines in modulating cancer cell stress and synergy with the combination of SMs may have an impact on sEV release. B16F10-OVA cells were treated under cytokine-conditioned settings, particularly TNFα and IFNβ. TNFα and IFNβ, have been previously studied to synergize with LCL 161[68,69]. Similar to my previous findings, SM treatment increased particle concentration relative to controls. The treatment of B16F10-OVA cells with IFNβ did not substantially increase sEV release and the combination with LCL161 did not result in an increase beyond LCL161 alone (**Figure 8D**). The same trend was seen when B16F10-OVA cells were

treated with TNFα; however, the combination of TNFα and LCL161 increased the sEV release by a factor of ~2.4 higher compared to vehicle controls.

In this experiment, I pre-treated B16F10-OVA cells with IFNγ 12-hours prior to LCL161 treatment and collected sEVs after 24 hour treatment with LCL161 (**Figure 8E**). The highest particle concentrations were observed in the IFNγ pre-treated LCL161 condition. This combination was seen to increase the release of these sEVs by a factor of ~40.4 compared to vehicle treatment. This shows that prior inflammatory conditioning may further synergize with LCL161 to release sEVs.

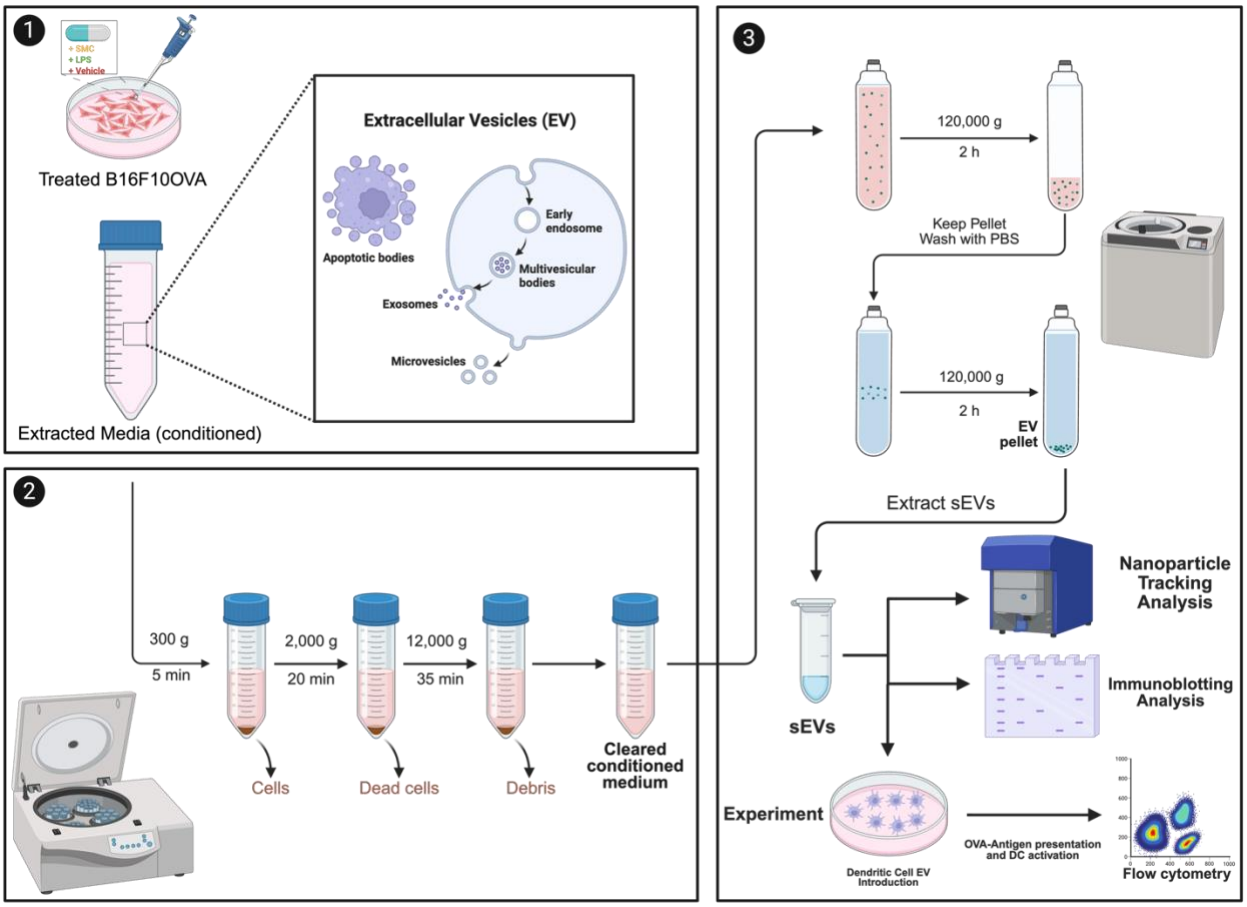

Figure 7. Experimental workflow for isolating and characterizing sEVs from cancer cells. Conditioned media from treated cancer cells is first subjected to sequential low-speed centrifugation to remove cells, dead cells, and large cellular debris. The clarified media is processed by ultracentrifugation at high speed to pellet sEV-enriched samples. The pellet washed with PBS and pelleted again via ultracentrifugation. The resulting sEV pellet is resuspended for downstream characterization and experimentation.

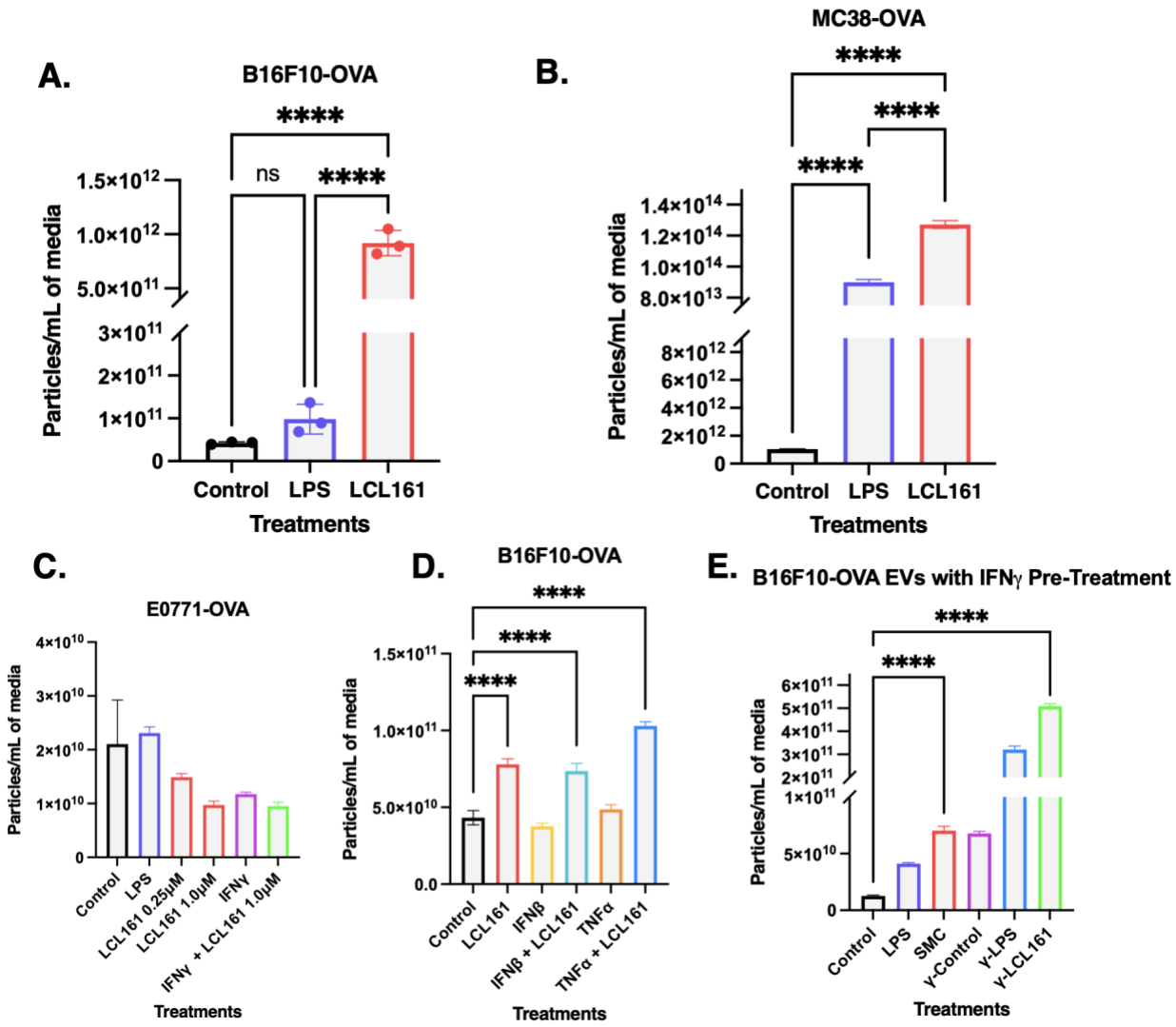

Figure 8. LCL161 increases EV release of resistant cancer cell lines but not sensitive cancer cells. (A, B) B16F10-OVA and MC38-OVA cells were treated with 2.5 μM LCL161, 1 μg/mL LPS, or vehicle (DMSO) for 24 hours. sEVs were then extracted via ultracentrifugation and were quantified through NTA (n=biological 3, technical 15, B16F10-OVA. n=1, technical 5, MC38-OVA). **(C)** E0771-OVA cells were treated with 2.5 μM LCL161, 1 μg/mL LPS, 250 U/mL of IFNγ, vehicle (DMSO) or combination for 24 hours. Note, IFNγ was done as a pre-treatment 12 hours before LCL161 or vehicle treatment. sEVs were then extracted via ultracentrifugation and were quantified through NTA (n=1, technical 5). **(D)** B16F10-OVA cells were treated with 2.5 μM LCL161, 1μg/mL LPS, 50 U/mL of IFNβ, 1n g/mL of TNFα, vehicle (DMSO) or combination for 24 hours. sEVs were then extracted via ultracentrifugation and were quantified through NTA (n=1, technical 5). **(E)** B16F10-OVA cells were treated with 2.5 μM LCL161, 1 μg/mL LPS, 250 U/mL of IFNγ, vehicle (DMSO) or combination for 24 hours. sEVs were then extracted via ultracentrifugation and were quantified through NTA (n=1, technical 5).

Characterization of tumour-derived sEVs suggest ESCRT-dependent mechanism of biogenesis.

I next evaluated the sEV size and cargo via NTA, TEM and western blotting. In B16F10-OVA cells, across the different treatment conditions, the size of the particles remained around the size of 100-150 nm (**Figure 5A**). This trend was similarly seen in both MC38-OVA and E0771-OVA cells (**Figure 5B** and **Figure 5C**). Therefore, LCL161 and combinations with or without different cytokines do not alter the size of the particles themselves. Further size analysis and visualization were sought by performing TEM on B16F10-OVA cancer cells, whereby the isolated sEVs are under 200 nm in diameter (**Figure 5D**).

The biogenesis pathway for sEVs was analyzed via immunoblotting. The sEVs derived from treated B16F10-OVA cells were positive for the ESCRT-dependent pathway markers TSG101 and Syntenin-1 and were negative for the Calnexin (marker of cellular contamination) (**Figure 5E**).

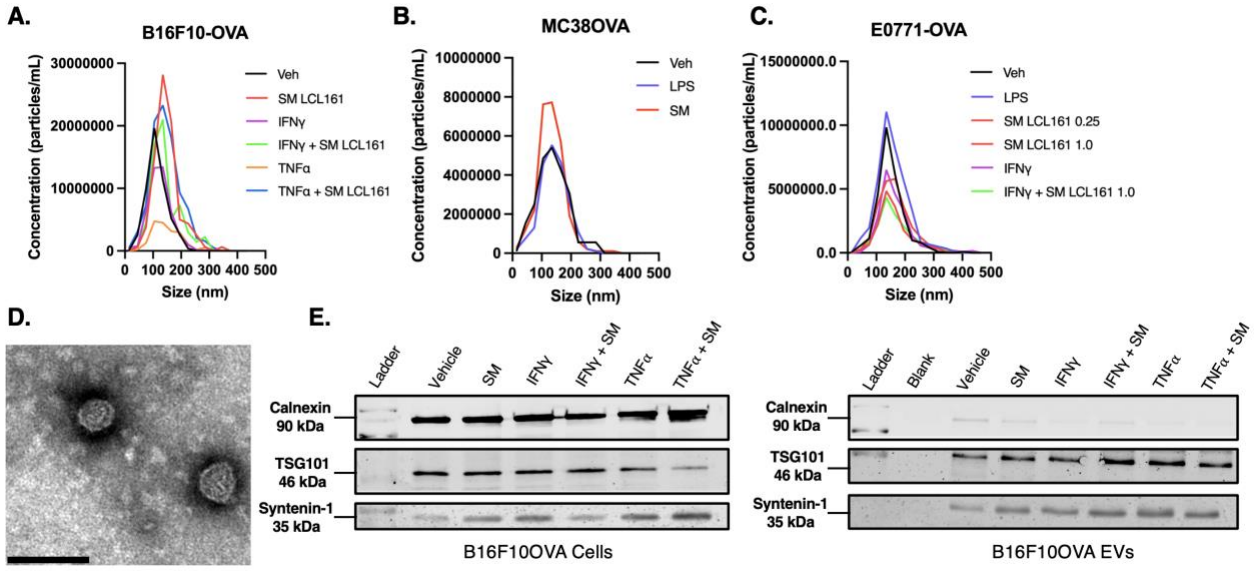

Figure 9. ESCRT-dependent sEV characterization through nanoparticle tracking analysis, transmission electron microscopy, and immunoblotting. (A-C) B16F10-OVA, MC38-OVA, and E0771-OVA were treated with 2.5 μM LCL161, 1μg/mL LPS, 250 U/mL of IFNγ, 1ng/mL of TNFα, vehicle (DMSO) or combination for 24 hours. Particle size distribution of sEVs collected are displayed from NTA results. **(D)** TEM image of vehicle treated B16F10-OVA sEVs that were negatively stained with uranyl acetate. Scale bar indicates 200 nm. **(E)** B16F10-OVA cells and B16F10-OVA sEVs were probed for the sEV markers Syntenin-1 and TSG101, while calnexin was assessed as a negative marker for cellular contamination.

3.2 Aim 2: Evaluate the effects of SM-treated sEVs on DCs and cytotoxic T cells

SMs and sEVs increase DC activation and antigen presentation

For these experiments, I incubated the DC cell line JAWSII with sEVs and/or LCL161 for 24 hours and then assessed for DC activation and antigen presentation via flow cytometry (**Figure 10A**). DC maturation is a critical step for effective antigen presentation and imitation of adaptive immune responses. Immature DCs typically display low expression of costimulatory molecules and have intracellular MHCII localization; whereas, in matured states, there is an increased surface expression of CD86 and MHCII[133,134]. The treatment of JAWSII with LCL161 led to an ~2.1 fold increase of activated DCs (**Figure 10B**), demonstrating that LCL161 can facilitate the maturation of DCs. Importantly, no differences in DC maturation were observed between different sEV origins, regardless of LCL161 treatment, suggesting that sEV source does not differentially modulate DC activation.

Antigen presentation was assessed compared to the positive control of DCs pulsed with the OVA peptide (SIINFEKL) and LPS. The treatment of JAWSII with LCL161 led to the most antigen presentation of MHCI bound OVA compared to all treatment groups (**Figure 10C**). Particularly, there was a fold increase of ~3.2, ~3.8, and ~4.9, for vehicle, LPS, and SM EV treatment groups when co-treated with LCL161, respectively, compared to the no EVs group. This pattern was also evident with sEVs derived from MC38-OVA cells. Notably, the highest antigen presentation of MHCI bound OVA was observed in the sEV and SM treated groups (**Figure 7D**). Particularly, there was a fold increase of ~5.8, ~4.7, and ~4.9, for vehicle, LPS, and SM EV treatment groups treated by LCL161, respectively, compared to no EVs.

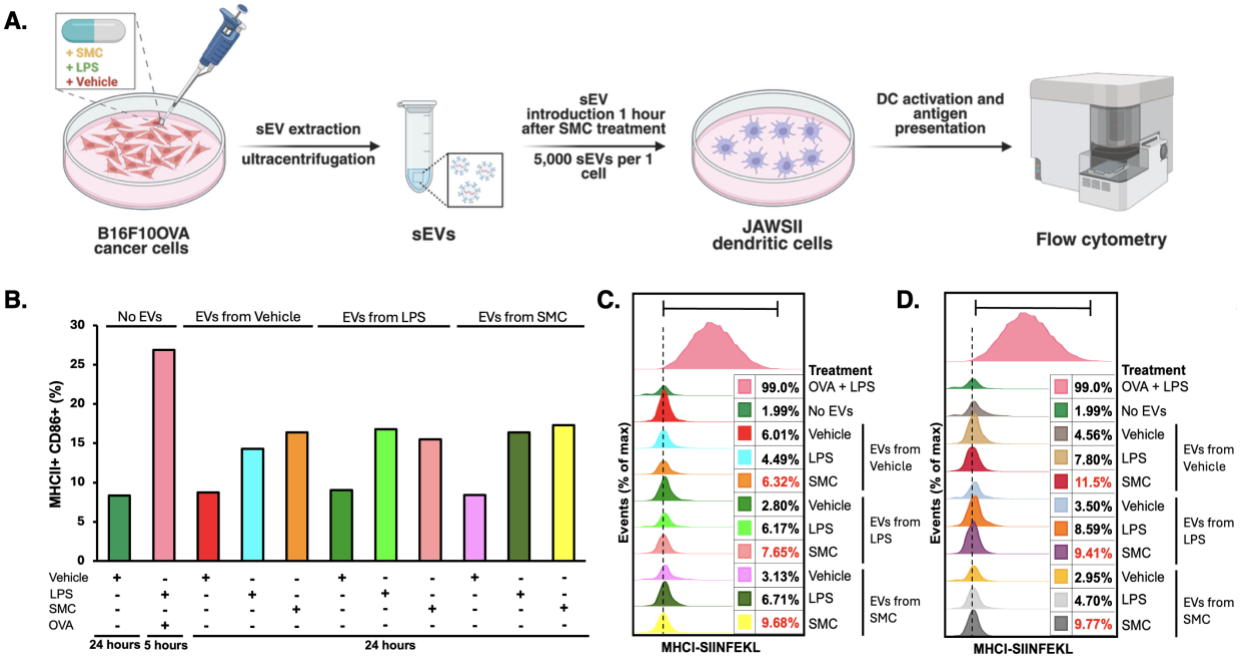

Figure 10. LCL161 enhances JAWSII activation and antigen presentation. (A) Experimental workflow for the testing of sEVs extracted from B16F10-OVA cells for DC activation and antigen presentation. JAWSII were pulsed for 24 hours at a ratio of 5,000 sEVs per cell along with vehicle, 1.0 μM LCL161, or 1μg/mL LPS (positive control). **(B)** DC activation was quantified as the percentage of $MHCII^+$ and $CD86^+$ cells. **(C, D)** DC antigen presentation of both B16F10-OVA sEVs and MC38-OVA sEVs was quantified as the percentage of MHCI-$SIINFEKL^+$ cells. Positive control for experiments was treating the JAWSII with 1 μg/mL LPS and 10 μg/mL SIINFEKL peptide without sEVs. (n=1)

SM-treated and sEV-pulsed JAWSII activate OVA-specific cytotoxic T cells

To assess the functional consequence of DC maturation on antigen presentation and subsequent T cell activation, I co-cultured OT-I T cells with sEV pulsed and SM treated JAWSII and then analyzed for OT-I T cell activation by $CD69^+$ surface presentation (**Figure 11A**). CD69 is used as an early maker of T cell activation as typical resting T cells display little CD69 expression. Once APCs interact with the TCR/CD3 pathway of the T cells, CD69 is rapidly increased on the cell surface[135]. In this experiment, we used IFNγ pre-treated B16F10-OVA sEVs that were also treated with LCL161, LPS, or vehicle. These IFNγ pre-treated sEVs were pulsed into JAWSII along with LCL161 24 hours prior to $CD8^+$ T cell co-culturing. After co-culture, IFNγ pre-treated sEVs with LCL161 displayed a 94.1%, 90.3%, and 96.5% (γvehicle, γLPS, γSM) increase in CD69 expression compared to the 98.6% of SIINFEKL pulsed positive control (**Figure 11B**). CD69 expression levels were also comparable to LPS treated groups as well.

Further activation and potential exhaustion of $CD8^+$ T cells were assessed by PD-1 surface presentation. PD-1 is commonly associated with T cell exhaustion; however, it is also known as a reflection of antigen-driven T cell stimulation[136,137]. After co-culture, IFNγ pre-treated sEVs with LCL161 displayed a 60.7%, 44.7%, and 62.4% (γvehicle, γLPS, γSM) increase in PD-1 expression on $CD8^+$ T cells, while SIINFEKL pulsed positive controls displayed 99.5% (**Figure 11C**).

Further, T cell proliferation was assessed by looking at the $CD3^+$ levels of the $CD8^+$ T cells. CD3 is a key component of the T cell receptor complex and functions as an intracellular signal-transducing module during T cell activation. In the past, T cell proliferation has been assessed through the use of anti-CD3 antibody stimulation along with IL-2[138]. A fold increase of ~1.9, ~1.5, and ~2.4 was observed for IFNγ pre-treated sEVs groups (vehicle, LPS, SM) with LCL161 and when compared to untreated group (**Figure 11D**).

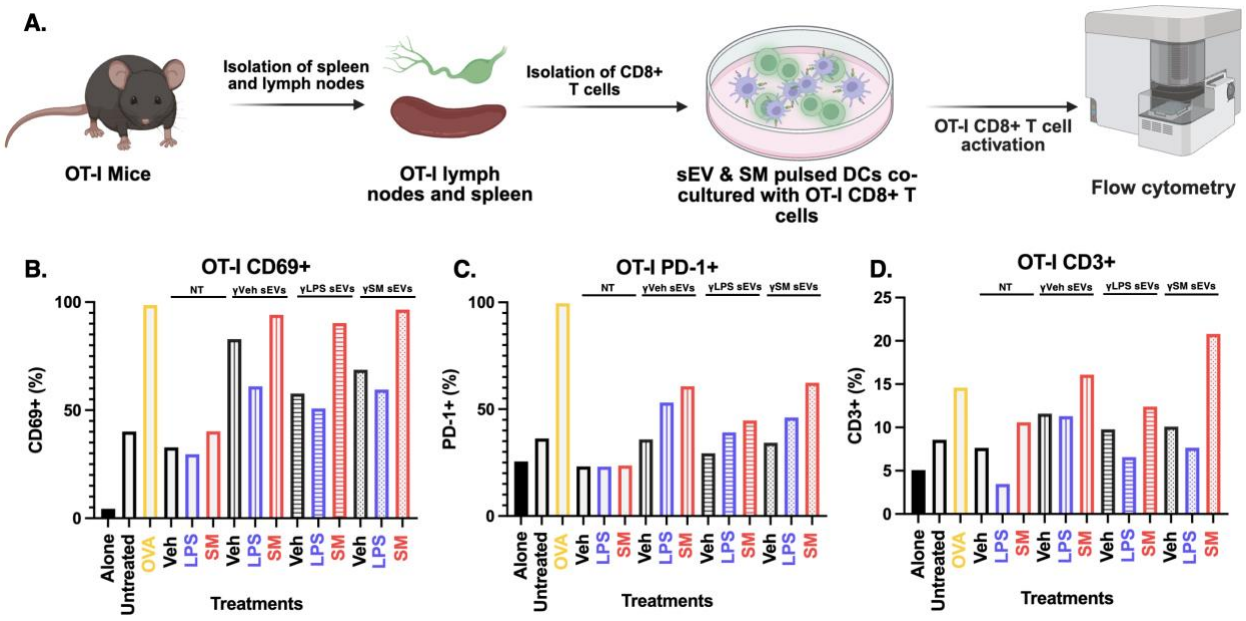

Figure 11. LCL161 and tumour derived sEVs enhance CD8$^+$ T cell activation. (A) Experimental workflow of OVA-specific CD8$^+$ T cell isolation and subsequent experiments. OT-I CD8$^+$ T cells were isolated from the spleens and lymph nodes of OT-I mice and co-cultured with sEV pulsed JAWSII to evaluate activation and proliferation. sEVs were isolated from B16F10-OVA cancer cells treated by various conditions. NT represents no treatment of sEVs. **(B)** T cell activation quantified as the percentage of CD69$^+$ T cells. T cells were co-cultured with B16F10-OVA pulsed sEVs JAWSII that were previously treated with 1.0 µM LCL161, 1 µg/mL LPS, or vehicle for 96 hours. Positive control for experiments was treating the JAWSII with 10µg/mL SIINFEKL peptide without sEVs. **(C)** T cell exhaustion and antigen driven activation was quantified as the percentage of PD-1$^+$ cells. **(D)** T cell proliferation was quantified as the percentage of CD3$^+$ cells. (n=1)

SMs and sEVs increase activation and antigen presentation in BMDCs

Since the JAWSII model is an immortalized DC cell line that may provide artificial results, I wanted to see the effects of the B16F10-OVA sEVs and LCL161 on primary BMDCs. BMDCs were isolated from the bone marrow of C57BL/6 mice using the technique of Inaba et al[139]. The isolated hematopoietic cells were differentiated with GM-CSF over seven days where they became immature BMDCs (**Figure 12A**). After 24 hours of incubating BMDCs with varying B16F10-OVA sEVs with or without LCL161, I then assessed DC viability, activation and antigen presentation via flow cytometry.

The assessment of BMDCs viability was via quantification of the proportion of live/dead cells (**Figure 12B**). Viability of BMDCs treated with 1.0 μM LCL161 is biologically insignificant as it did not majorly decrease compared to vehicle, positive, and untreated. This indicates that the treatment conditions are not overtly toxic to BMDCs.

BMDC activation was quantified by calculating the proportion of $MHCII^+/CD86^+$ cells. In contrast to the JAWSII results, treatment of BMDCs with LCL161 resulted in an increased factor of ~1.2 of activated BMDCs when compared to vehicle treatment alone (**Figure 12C**). However, the rate of maturation between vehicle and LCL161 of the same sEV group did not change significantly. On a similar basis, there was no difference in antigen presentation relative to control group (**Figure 12D**).

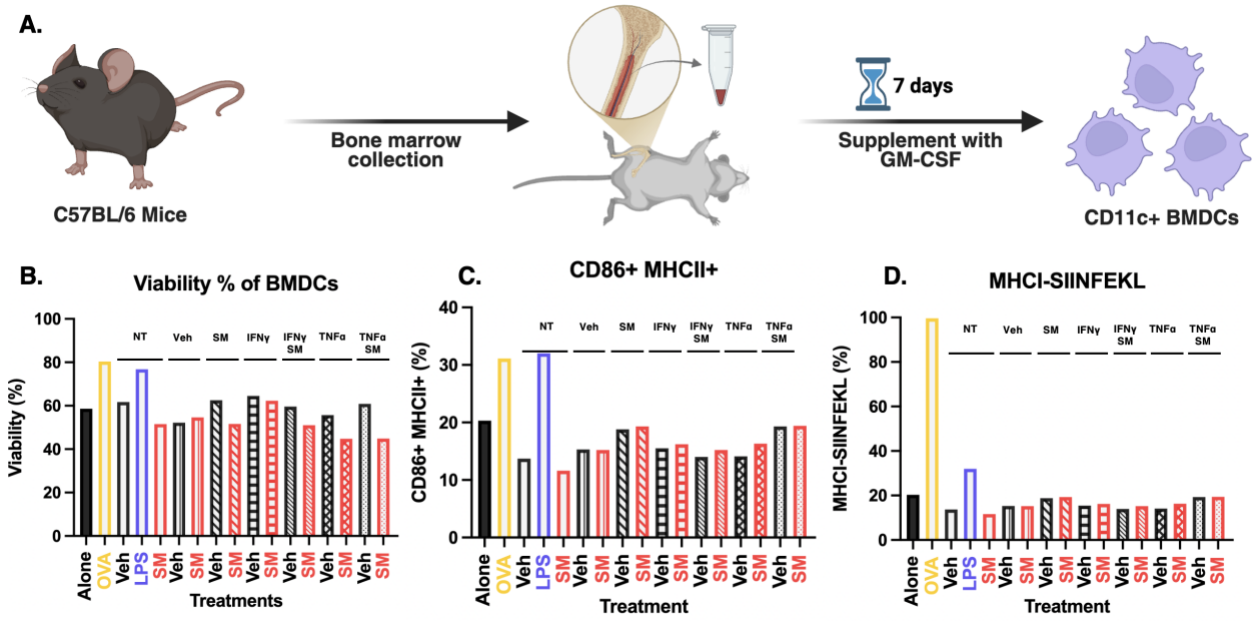

Figure 12. LCL161 enhances BMDC activation, but not antigen presentation when pulsed with tumour sEVs. (A) Experimental workflow of BMDC generation. Bone marrow was collected from C57BL/6 mice and further differentiated with GM-CSF where it was used for downstream experiments. NT represents no treatment with sEVs. **(B)** sEVs were isolated from B16F10-OVA cancer cells. BMDCs were treated with the isolated sEVs at a ratio of 5,000 sEVs per cell along with 1.0 µM LCL161, 1 µg/mL LPS, or vehicle for 24 hours. **(C)** DC activation was quantified as the percentage of $MHCII^+$ and $CD86^+$ cells. **(D)** DC antigen presentation of both B16F10-OVA sEVs and MC38-OVA sEVs, respectively, was quantified as the percentage of MHCI-$SIINFEKL^+$ cells. Positive control for experiments was treating the BMDCs with 1µg/mL LPS and 10 µg/mL SIINFEKL peptide without sEVs. (n=1)

SM-treated and sEV-pulsed BMDCs activate OVA-specific cytotoxic T cells

Despite the discouraging results with the BMDC results in **Figure 12**, we nevertheless assessed for OT-I activation in sEV pulsed and SM treated BMDCs. Surprisingly, there was a decrease in OT-I viability in all conditions with LCL161 treatment (**Figure 13A**). This was unlike JAWSII, where viability was consistent in terms of LCL161 versus vehicle treatment.

The activation of $CD8^+$ T cells was assessed by $CD69^+$ surface presentation. I used a variety of different treatment conditions pertaining to the source of B16F10-OVA sEVs. After co-culture of OT-I cells along with sEV-pulsed BMDCs and treatment with SM, the sEVs with LCL161groups displayed a 23.8%, 17.4%, 30.4%, 30.9%, 27.4%, and 27.7% (vehicle, SM, IFNγ, IFNγ + SM, TNFα, and TNFα + SM) increase in CD69 expression compared to the 32.8% of SIINFEKL pulsed positive control (**Figure 13B**).

Further, activation and potential exhaustion of $CD8^+$ T cells were assessed by PD-1 surface presentation. After co-culture, OT-I $CD8^+$ T cells displayed a 44.3%, 54.0%, 55.2%, 47.3%, 42.5%, and 49.4% (vehicle, SM, IFNγ, IFNγ + SM, TNFα, and TNFα + SM) increase in PD-1 expression on $CD8^+$ T cells, while SIINFEKL pulsed positive controls displayed 67.0% (**Figure 11C**).

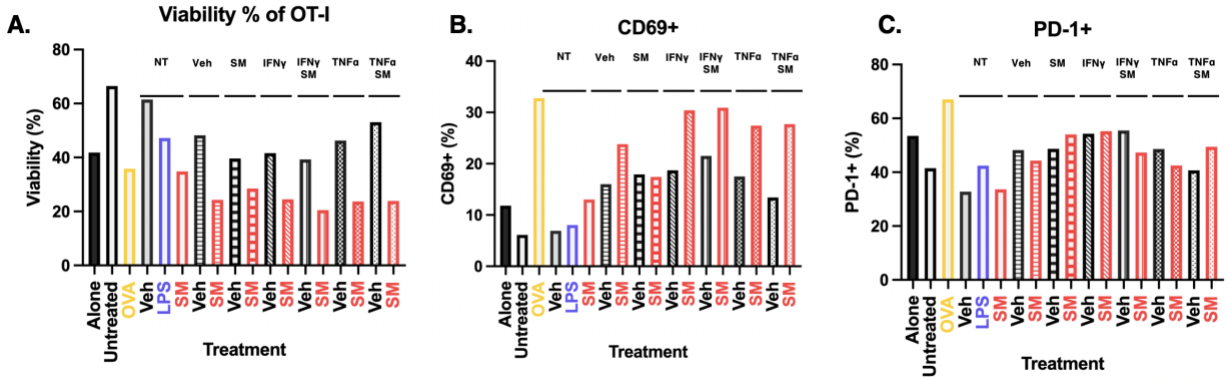

Figure 13. LCL161 and tumour derived sEVs enhances CD8$^+$ T cell activation but decrease viability in T cells. (A) T cell viability quantified as the percentage of live/dead T cells. T cells were co-cultured with B16F10-OVA pulsed sEV BMDCs that were previously treated with 1.0 µM LCL161, or vehicle for 96 hours. **(B)** T cell activation quantified as the percentage of CD69$^+$ T cells. Positive control for experiments was treating the BMDCs with 10 µg/mL SIINFEKL peptide without sEVs. **(C)** T cell exhaustion and antigen driven activation was quantified as the percentage of PD-1$^+$ cells. (n=1)

CHAPTER FOUR: DISCUSSION

4.1 SM sensitivity is cell line- and cytokine-dependent

SM sensitivity in the context of viability of both cancer cell lines and DCs can be seen as variable and cell line dependent. Thus SM sensitivity is heavily context-dependent, shaped by the survival signaling framework of each cell type[140]. In cancer cells, SMs promote the degradation of cIAP1/2 and shift TNFα signaling from pro-survival to pro-apoptotic NF-κB signaling. This allows RIPK1- and caspase-8-associated cell death, providing a rationale behind why the synergy of LCL161 and TNFα treatment can enhance cytotoxicity in LLC and MC38 models[69,140,141]. Moreover, a previous study showed that IFNγ can synergize with SM to induce cancer cell death through mechanisms independent of TNFα signaling[142]; further showing that viability patterns are not solely due to drug potency, but also evidence that cytokine exposure can reveal distinct weaknesses in certain IAP-regulated pathways. Overall, this can be further applied in the context of the TME, where SM treatment would function as sensitizing pressure, while the surrounding inflammatory environment determines whether the tumour survives or undergoes programmed cell death.

4.2 E0771 cancer cells display intrinsic sensitivity to low dose SM treatment

Through these experiments, E0771 cells have a heightened sensitivity towards varying doses of LCL161, further suggesting that this tumour line may possess an intrinsic dependence on IAP-regulated survival pathways. This experiment was consistent with a study showing that a subset of human cancer cell lines undergo apoptosis following SM monotherapy due to endogenous death signals, such as autocrine TNFα[140]. This is experimentally relevant in this research project as a highly sensitive cell line may generate EVs under conditions of substantial cellular stress or death, which would in turn alter particle abundance and associated cargos[143].

4.3 SM increases tumour-derived sEV release without affecting size distribution

Interestingly, SM exposure promotes EV production in B16F10-OVA and MC38-OVA; however, it does not decrease the viability of the cells after treatment. Treatment with SM suggests that IAP antagonism may alter cancer cell secretory behaviour. Previous studies have shown that stress-associated pathways, such as p53-dependent signaling, can increase sEV secretion through TSAP6 mechanisms[144]. The confirmation of sEV size was done not only using NTA, but were further interpreted with TEM and western blotting[131,132,145]. Additionally, with western blotting, ESCRT-dependent biogenesis of sEVs can be deduced. Future directions would be to explore regulated vesicle biogenesis and cellular stress responses. This can be done through loss-of-function experiments targeting Rab27a and Rab27b, as it has been shown that Rab GTPases promote sEV secretion in cancer cells[146]. Moreover, LPS served as a positive control due to its well-established inflammatory effects and known outcome to enhance sEV release. Through the activation of TLR4, LPS can engage NF-κB/IKK-associated pathways and promote sEV secretion[147]. This further supports the hypothesis that due to how SM treatment, through its ability to remodel intracellular signaling, promotes activation of the non-canonical NF-κB pathway and induce interferon-associated transcriptional programs[148]. Thus, active inflammatory reprogramming may play a role in sEV release for these resistant cancer cells.

To further address the lack of sEV production under LCL161 circumstances for E0771 cells, it can be due to their heightened sensitivity towards SMs. Since SMs can induce rapid degradation of cIAP proteins within the first few hours of treatment, cancer cell death occurs between 18 to 24 hours for sensitive cell lines[149–151]. Thus, reductions in sEV recovery following SM treatment may be low or comparable to vehicle treatment as massive amounts of cell death occurs within the first

2-18 hours of treatment. Further directions would be to normalize the particle secretion to viable cells and explore the potential of altered EV-release and biogenesis pathways.

4.4 Tumour-derived sEVs with SMs may enhance DC activation and antigen presentation

When comparing the results from JAWSII, an immortalized dendritic cell line, compared to BMDCs, a primary dendritic cell line, we see generally the same trends; however, differences in the amount of expression on the surface of the cells. Looking at $MHCII^+$ and $CD86^+$ dendritic cells, both JAWSII and BMDCs exhibited increased expression compared to vehicle control. One difference noticed was that the levels of MHCII and CD86 were similar in expression level for varying sEVs that were treated with vehicle or SM. BMDCs were differentiated from GM-CSF, thus they are a heterogeneous primary culture containing DC-like cells and macrophage-like populations. This can shift levels of MHCII and CD86 expression without changing the overall direction of the response[152]. Further, studies have shown that tumour-derived sEVs can regulate DC maturation at the costimulatory stage, suggesting that sEVs can have effects on DC phenotype that are not always linearly reflected by MHCII and CD86[153]. As said, SM can directly promote DC maturation in some immune cell contexts, however these effects may be greater in altering cytokine output, antigen processing, and T cell stimulatory function rather than MHCII and CD86 levels[154,155]. Thus, evaluating the ability of sEV-pulsed DCs that were co-treated with vehicle or SM and its ability to elicit T cell activation would be a better predictor. Similarly, the lower antigen presentation may reflect the heterogeneity and variable maturation state of primary GM-CSF-derived cultures. A previous study showed that mature DCs that are pulsed with OVA-bearing sEVs displayed increased peptide MHCI, MHCII, and co-stimulatory molecule expression, and $CD8^+$ T cell responses compared to OVA-pulsed immature DCs[156]. Thus, antigen presentation is

dependent on the state of the DC. This may reflect the differences in sEV uptake and intracellular routing between JAWSII and BMDCs.

4.5 SM-treated tumour sEVs promote CD8$^+$ T cell activation, but may also affect T cell viability

In the JAWSII and OT-I T cell co-culture system, several sEV-treated and drug co-treatment conditions increased the proportion of CD69$^+$ CD8$^+$ T cells relative to untreated or vehicle-associated conditions, suggesting that DCs exposed to tumour-derived sEVs can provide early activation signals to antigen-specific CD8$^+$ T cells. CD69 has been validated as a proven method to measure T cell activation after antigenic stimulation[157]. The increase in CD69$^+$ was most apparent in conditions involving SM-associated sEVs and SM-treated DCs, supporting the explanation that SM exposure alters the activation state of the DC presenting said signals[155]. Further, the reduced surface CD3 expression observed on CD8$^+$ T cells may reflect activation-associated CD3/TCR downmodulation rather than a loss of T cell identity. A primary study demonstrated that peptide MHC stimulation induces downmodulation of the TCR-CD3 complex on CD8$^+$ T cells, with greater CD3 downmodulation associated with stronger functional avidity[158].

In parallel, PD-1 expression was increased across several activated JAWSII co-culture conditions, indicating that CD8$^+$ T cells were not only activated, but also may be initiating inhibitory feedback pathways downstream of antigen receptor engagement. A previous study showed that PD-1 are induced on stimulated T cells following in vitro activation with anti-CD3, reflecting recent activation rather than exhaustion alone[159]. However, it is important to acknowledge that PD-1 expression has also been associated with dysfunctional or exhausted CD8$^+$ T cell states during chronic antigen exposure. As an example, during times of chronic viral

infection, PD-1 blockade restores function in exhausted $CD8^+$ T cells, suggesting that future experiments can utilize anti-PD-1/PD-L1 inhibitors in combination with tumour-derived sEVs and SM[160,161].

In the BMDC and OT-I T cell co-culture system, CD69 expression is also increased in sEV-treated and SM-associated conditions, suggesting that the activation phenotype observed with JAWSII cells are also physiologically relevant with the use of primary cells. Unlike JAWSII, the BMDC co-culture experiment showed a notable reduction in OT-I viability across several treatment conditions, particularly in groups that had BMDCs receive LCL161. This suggests that activation and loss of T cell fitness may occur when exposed to LCL161. A previous study has shown that SMs can inhibit human T cell proliferation and may not uniformly enhance T cell effector function[162]. However, in this experiment, SM was not applied directly to the $CD8^+$ T cells, suggesting that the observed reduction in T cell viability may reflect an indirect or secondary effect of the treatment conditions rather than direct SM-mediated cytotoxicity.

This dual effect is consistent with the broader biological effects of SMs, which can promote anti-tumour T cell responses in certain immune contexts while also directly altering cell survival and function depending on cell type, dose, and combinational cytokines[69,163]. Future directions would be to explore a washout assay as well as a viability assay for BMDC and OT-I co-culture experiments.

4.5.1 IFNγ pre-treatment increases $CD8^+$ T cell activation

IFNγ pre-treatment appeared to further increase $CD69^+$ OT-I cells in both JAWSII and BMDC co-culture systems. This suggests that inflammatory priming of cancer cells enhances the ability of DCs to stimulate antigen-specific $CD8^+$ T cell activation. IFNγ is known to induce MHC

expression[164]. Thus, treatment of IFNγ on cancer cells in combination with LCL161 may elicit greater T cell activation. Further, IFNγ may be able to present at a higher expression level of MHCI on tumour-derived sEVs[165]. As well, IFNγ can induce MHCI upregulation in cancer cells, further supporting the possibility that IFNγ-conditioned tumour-derived EVs may be more efficiently recognized in downstream immune assays[166]. Overall, this model remains consistent with previous publication that tumour-derived EVs can provide antigenic material for cytotoxic T cell cross-priming and how IFNγ is able to improve overall MHC expression[167].

4.6 Limitations to study

Overall, this study provided important evidence that SM treatment may influence tumour-derived sEV release, DC antigen presentation, and downstream $CD8^+$ T cell activation; however, there are several limitations that should be addressed when interpreting these findings.

In terms of biological replicates, much of the work was performed using only a single biological replicate. This limits the ability to determine whether the observed changes are reproducible across independent experiments or statistically significant

Another limitation is that this project utilizes LCL161, a monovalent SM. There are many different types of SMs ranging from varied monovalent, such as LCL161, AT-406, GDC-0152, and bivalent SMs such as Birinapant, BV6, and SM-164[168–170]. It is important to note that SMs can vary in their affinity, potency, and ability to degrade cIAP1/2 and XIAP. This means that the observed effects on sEV release and immune activation may be compound- and dose-dependent. With this, it is important to acknowledge that different concentrations may impact the amount of sEV release. Thus, it is important for a future direction of this study to also use a range of

concentrations to validate the selected concentration of LCL161 for sEV release, DC activation, and T cell stimulation.

Furthermore, restricting the analysis to a single tumour model also has its limits in interpretation of the findings as cancer cells are heterogenous in their sensitivity to SMs, antigen expression, and EV-cargo. It is important for the study to also look at the effects of T cell activation in semi-sensitive and sensitive models, such as the MC38, LLC, and E0771 cells.

The OVA/OT-I system is another limitation. This systems allows a highly controlled antigen-specific model that may not fully reflect endogenous tumour antigen recognition[171]. Aspects such as effector differentiation, memory formation, and expansion kinetics can be altered with TCR-transgenic $CD8^+$ T cells[171]. Thus, future *in vivo* studies should include SIINFEKL tetramer or dextramer staining, and non-OVA tumour controls.

4.7 Future directions

4.7.1 Evaluate the potential synergistic effects of SMs and immune cell derived sEVs

To extend the potential of sEVs in the context of cancer therapeutics, it would be informative to evaluate whether SM treatment can enhance the immunostimulatory function of immune cell-derived sEVs. More specifically, analyzing the effects of DC-derived sEVs that have been exposed to tumour-derived sEVs and SM or combination therapies. In literature, it is already known that DC derived vesicles can induce antigen-specific $CD8^+$ T cell responses in vivo[168]. By being able to pulse BMDCs with tumour-derived sEVs and use SMs to contribute to the maturation and potentially increase sEV release will allow a robust approach in activating $CD8^+$ T cells[173,174].

It has been shown that mature DCs that have been pulsed with sEVs elicit a more robust $CD8^+$ T cell response[175]. Thus, it would be beneficial to compare sEV pulsing on immature BMDCs, mature BMDCs, to SM-treated BMDCs.

Moreover, $CD8^+$ T cell-derived sEVs should be explored as activated T cells can release vesicles carrying TCR/CD3-associated signaling complexes and adhesion molecules, further suggesting that these EVs may participate in immune communication beyond direct T cell contact[176,177]. Isolating sEVs from OT-I cells after co-culture with SM-treated sEV-pulsed BMDCs would determine whether these activated T cells are able to release functionally active immune sEVs. These sEVs could then be assessed for cytotoxic cargo such as, granzyme B, and tested to see eradication of SM resistant and sensitive tumours (**Figure 14**)[178].

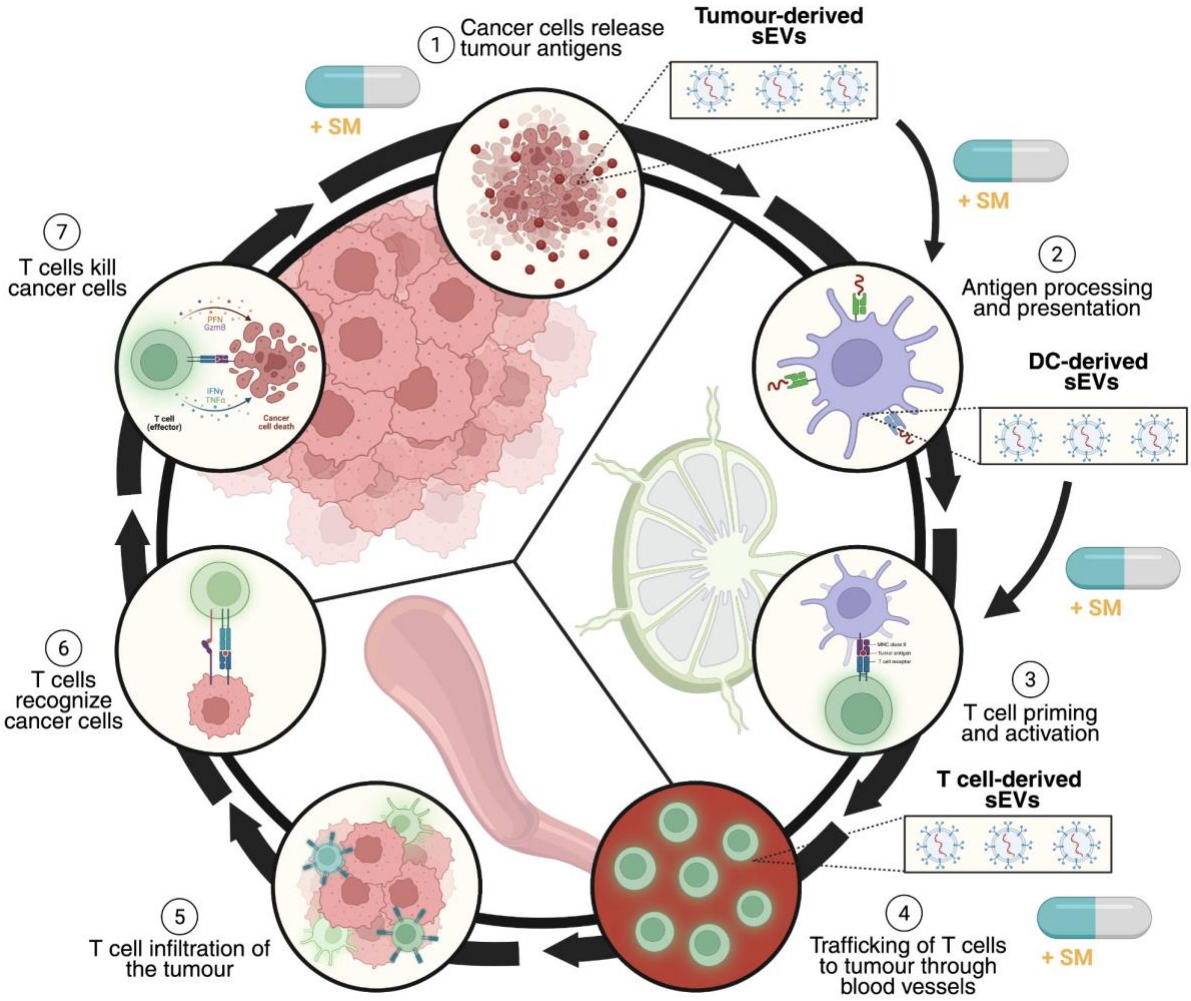

Figure 14. Modified overview of the CI cycle highlighting the role of SMs and sEVs. Tumour cell death releases antigens that are captured by DCs, a process enhanced by SMs through increased tumour cell killing and antigen availability, while tumour-derived sEVs can also possess tAgs and immunomodulatory signals. SMs promote DC maturation, improving antigen processing and presentation, and may also influence the immunogenic cargo of DC- and tumour-derived sEVs. These effects enhance T cell priming and activation, with sEVs further contributing to intercellular communication across the cycle. Finally, SMs sensitize tumour cells to apoptosis and support T cell mediated killing, reinforcing the CI cycle.

4.7.2 Proposed *in vivo* model for therapeutic evaluation of SM-treated tumour sEV-pulsed BMDCs

Extending past the in vitro findings, a proposed in vivo model will provide more insight in physiologically relevant settings. Due to the potential of DC therapies, exploring tumour sEV-pulsed BMDCs can mediate anti-tumour immunity against OVA-expressing syngeneic tumours would be interesting as both a prophylactic and therapeutic model. This approach has been studied in previous work displaying that tumour-derived sEVs can transfer tumour antigens to DCs, which then cross-prime $CD8^+$ cytotoxic T cells and mediate anti-tumour effects in vivo[179]. This model would include isolated sEVs from SM-treated B16F10-OVA, E0771-OVA, LLC-OVA, and MC38-OVA cells being applied to BMDCs that are also exposed to LCL161. This would allow for BMDC maturation and activation, while also increasing antigen presentation. Further, the synergistic use of IFNγ pre-treatment and LCL161 can be utilized to provide a more robust $CD8^+$ T cell activation.

To test this, C57BL/6 mice will receive intravenous administration of BMDCs pulsed with sEVs derived from corresponding tumour models. The timeline will be representative of Wang et al., as multiple intravenous administrations will allow a boost of anti-tumour immunity[180]. This will be done in parallel to appropriate controls such as using a non-OVA-expressing wild type to distinguish antigen-dependent immunity as well as PBS administrations as a negative control. Primary assessments of mice would include tumour growth kinetics and overall survival. Further frequency of OVA-specific $CD8^+$ T cells and broader phenotyping of tumour-infiltrating and lymphoid immune populations will be assessed by flow cytometry.

It is anticipated that BMDCs that are exposed to sEVs from SM-treated cancer cells and paired with the LCL161 treatment, will generate a stronger anti-tumour immunity compared to controls. Furthermore, the comparison of vehicle-derived sEVs and SM-derived sEVs can be done. If it shows that SM-derived sEVs has an increased OVA-specific $CD8^+$ T cell response, it suggests that

SM treatment alters tumour-derived sEVs in a way that improves their ability to support antigen presentation in downstream T cell priming.

4.8 Conclusion

Overall, this study suggests that SM treatment does not produce a uniform effect across all tumour and immune cell models, but instead alters the viability, sEV release, DC antigen presentation, and $CD8^+$ T cell activation in a context-dependent manner. While there are some cell lines that are semi-sensitive or sensitive to SM, others respond through altered sEV release and enhanced immune crosstalk, further supporting the idea of SM as an agent of immune modulators rather than just an anti-cancer drug. These findings serve as a foundation for a proposed model in which SM-treated tumour cells release immunologically altered sEVs that are taken up by DCs, leading to improved antigen presentation and early activation of tumour-specific $CD8^+$ T cells. Future work should determine whether molecular cargo within these sEVs and its translation towards a durable anti-tumour immunity in vivo. Thus, this thesis supports a broader framework in which SMs and sEVs may be integrated into a novel immunotherapeutic strategy.

REFERENCES

1. Gonzalez, H., Hagerling, C. & Werb, Z. Roles of the immune system in cancer: from tumor initiation to metastatic progression. *Genes Dev.* **32**, 1267–1284 (2018).

2. Sung, H. *et al.* Global Cancer Statistics 2020: GLOBOCAN Estimates of Incidence and Mortality Worldwide for 36 Cancers in 185 Countries. *CA: A Cancer Journal for Clinicians* **71**, 209–249 (2021).

3. Poirier, A. E. *et al.* The future burden of cancer in Canada: Long-term cancer incidence projections 2013–2042. *Cancer Epidemiology* **59**, 199–207 (2019).

4. Yabroff, K. R., Gansler, T., Wender, R. C., Cullen, K. J. & Brawley, O. W. Minimizing the burden of cancer in the United States: Goals for a high-performing health care system. *CA: A Cancer Journal for Clinicians* **69**, 166–183 (2019).

5. Simmons, L. A. Self-perceived burden in cancer patients: validation of the Self-perceived Burden Scale. *Cancer Nurs* **30**, 405–411 (2007).

6. Marusak, H. A. *et al.* Emotion-related brain organization and behavioral responses to socioemotional stimuli in pediatric cancer survivors with posttraumatic stress symptoms. *Pediatric Blood & Cancer* **66**, e27470 (2019).

7. Hanahan, D. Hallmarks of Cancer: New Dimensions. *Cancer Discov* **12**, 31–46 (2022).

8. Tiwari, A., Trivedi, R. & Lin, S.-Y. Tumor microenvironment: barrier or opportunity towards effective cancer therapy. *J Biomed Sci* **29**, 83 (2022).

9. Sounni, N. E. & Noel, A. Targeting the Tumor Microenvironment for Cancer Therapy. *Clin Chem* **59**, 85–93 (2013).

10. Simsek, H. & Klotzsch, E. The solid tumor microenvironment—Breaking the barrier for T cells. *BioEssays* **44**, 2100285 (2022).

11. Cairns, R., Papandreou, I. & Denko, N. Overcoming Physiologic Barriers to Cancer Treatment by Molecularly Targeting the Tumor Microenvironment. *Mol Cancer Res* **4**, 61–70 (2006).

12. Jing, X. *et al.* Role of hypoxia in cancer therapy by regulating the tumor microenvironment. *Mol Cancer* **18**, 157 (2019).

13. Hartupee, C. *et al.* Pancreatic cancer tumor microenvironment is a major therapeutic barrier and target. *Front. Immunol.* **15**, (2024).

14. Gajewski, T. F., Schreiber, H. & Fu, Y.-X. Innate and adaptive immune cells in the tumor microenvironment. *Nat Immunol* **14**, 1014–1022 (2013).

15. Galli, F. *et al.* Relevance of immune cell and tumor microenvironment imaging in the new era of immunotherapy. *J Exp Clin Cancer Res* **39**, 89 (2020).

16. Tiwari, A. *et al.* Towards a consensus definition of immune exclusion in cancer. *Front Immunol* **14**, 1084887 (2023).

17. Lei, X. *et al.* Immune cells within the tumor microenvironment: Biological functions and roles in cancer immunotherapy. *Cancer Letters* **470**, 126–133 (2020).

18. Zhou, Y., Chen, X., Cao, J. & Gao, H. Overcoming the biological barriers in the tumor microenvironment for improving drug delivery and efficacy. *Journal of Materials Chemistry B* **8**, 6765–6781 (2020).

19. Zinatizadeh, M. R. *et al.* The Nuclear Factor Kappa B (NF-kB) signaling in cancer development and immune diseases. *Genes & Diseases* **8**, 287–297 (2021).

20. Dolcet, X., Llobet, D., Pallares, J. & Matias-Guiu, X. NF-kB in development and progression of human cancer. *Virchows Arch* **446**, 475–482 (2005).

21. Lalle, G. *et al.* NF-κB subunits RelA and c-Rel selectively control CD4+ T cell function in multiple sclerosis and cancer. *J Exp Med* **221**, e20231348 (2024).

22. Kabacaoglu, D., Ruess, D. A., Ai, J. & Algül, H. NF-κB/Rel Transcription Factors in Pancreatic Cancer: Focusing on RelA, c-Rel, and RelB. *Cancers (Basel)* **11**, 937 (2019).

23. Inoue, J.-I., Gohda, J., Akiyama, T. & Semba, K. NF-kappaB activation in development and progression of cancer. *Cancer Sci* **98**, 268–274 (2007).

24. Park, H. H. Structure of TRAF Family: Current Understanding of Receptor Recognition. *Front Immunol* **9**, 1999 (2018).

25. Kim, Y.-S., Schwabe, R. F., Qian, T., Lemasters, J. J. & Brenner, D. A. TRAIL-mediated apoptosis requires NF-kB inhibition and the mitochondrial permeability transition in human hepatoma cells. *Hepatology* **36**, 1498–1508 (2002).

26. Wallach, D. Cell death induction by TNF: a matter of self control. *Trends Biochem Sci* **22**, 107–109 (1997).

27. Maldonado, M. E., Bousserouel, S., Gossé, F., Lobstein, A. & Raul, F. Implication of NF-κB and p53 in the expression of TRAIL-death receptors and apoptosis by apple procyanidins in human metastatic SW620 cells. (2010).

28. Moneva-Sakelarieva, M. *et al.* The role of the transcription factor NF-kB in the pathogenesis of inflammation and carcinogenesis. Modulation capabilities. *Pharmacia* **72**, 1–13 (2025).

29. Liu, T., Zhang, L., Joo, D. & Sun, S.-C. NF-κB signaling in inflammation. *Sig Transduct Target Ther* **2**, 17023 (2017).

30. Arlıer, S., Kayışlı, Ü. A. & Arıcı, A. Tumor necrosis factor alfa and interleukin 1 alfa induced phosphorylation and degradation of inhibitory kappa B alpha are regulated by estradiol in endometrial cells. *Turk J Obstet Gynecol* **15**, 50–59 (2018).

31. Santini, D. *et al.* Receptor activator of NF-kB (RANK) expression in primary tumors associates with bone metastasis occurrence in breast cancer patients. *PLoS One* **6**, e19234 (2011).

32. Zhang, L. *et al.* Function of phosphorylation of NF-kB p65 ser536 in prostate cancer oncogenesis. *Oncotarget* **6**, 6281–6294 (2015).

33. Hai Ping, P., Feng Bo, T., Li, L., Nan Hui, Y. & Hong, Z. IL-1β/NF-kb signaling promotes colorectal cancer cell growth through miR-181a/PTEN axis. *Arch Biochem Biophys* **604**, 20–26 (2016).

34. Yenmis, G. *et al.* Anti-cancer effect of metformin on the metastasis and invasion of primary breast cancer cells through mediating NF-kB activity. *Acta Histochemica* **123**, 151709 (2021).

35. Baldwin, A. S. Regulation of cell death and autophagy by IKK and NF-κB: critical mechanisms in immune function and cancer. *Immunological Reviews* **246**, 327–345 (2012).

36. Wu, X., Sun, L. & Xu, F. NF-κB in Cell Deaths, Therapeutic Resistance and Nanotherapy of Tumors: Recent Advances. *Pharmaceuticals (Basel)* **16**, 783 (2023).

37. Véquaud, E. *et al.* YM155 potently triggers cell death in breast cancer cells through an autophagy-NF-kB network. *Oncotarget* **6**, 13476–13486 (2015).

38. Cetraro, P., Plaza-Diaz, J., MacKenzie, A. & Abadía-Molina, F. A Review of the Current Impact of Inhibitors of Apoptosis Proteins and Their Repression in Cancer. *Cancers* **14**, 1671 (2022).

39. LaCasse, E. C., Baird, S., Korneluk, R. G. & MacKenzie, A. E. The inhibitors of apoptosis (IAPs) and their emerging role in cancer. *Oncogene* **17**, 3247–3259 (1998).

40. Fan, H. *et al.* The critical role of X-linked inhibitor of apoptosis protein (XIAP) in tumor development. *Apoptosis* **30**, 1202–1215 (2025).

41. Hunter, A. M., LaCasse, E. C. & Korneluk, R. G. The inhibitors of apoptosis (IAPs) as cancer targets. *Apoptosis* **12**, 1543–1568 (2007).

42. Lalaoui, N. & Vaux, D. L. Recent advances in understanding inhibitor of apoptosis proteins. *F1000Res* **7**, F1000 Faculty Rev-1889 (2018).

43. Liston, P. *et al.* Suppression of apoptosis in mammalian cells by NAIP and a related family of IAP genes. *Nature* **379**, 349–353 (1996).

44. Bai, L., Smith, D. C. & Wang, S. Small-molecule SMAC mimetics as new cancer therapeutics. *Pharmacology & Therapeutics* **144**, 82–95 (2014).

45. Kipp, R. A. *et al.* Molecular Targeting of Inhibitor of Apoptosis Proteins Based on Small Molecule Mimics of Natural Binding Partners. *Biochemistry* **41**, 7344–7349 (2002).

46. Mace, P. D., Shirley, S. & Day, C. L. Assembling the building blocks: structure and function of inhibitor of apoptosis proteins. *Cell Death Differ* **17**, 46–53 (2010).

47. Oberoi-Khanuja, T. K., Murali, A. & Rajalingam, K. IAPs on the move: role of inhibitors of apoptosis proteins in cell migration. *Cell Death Dis* **4**, e784 (2013).

48. Oberoi-Khanuja, T. K., Murali, A. & Rajalingam, K. IAPs on the move: role of inhibitors of apoptosis proteins in cell migration. *Cell Death Dis* **4**, e784–e784 (2013).

49. Chen, D. J. & Huerta, S. Smac mimetics as new cancer therapeutics. *Anticancer Drugs* **20**, 646–658 (2009).

50. Wang, S. Design of small-molecule Smac mimetics as IAP antagonists. *Curr Top Microbiol Immunol* **348**, 89–113 (2011).

51. Wang, Y. *et al.* Complex IIa formation and ABC transporters determine sensitivity of OSCC to Smac mimetics. *Cell Death Dis* **15**, 1–15 (2024).

52. Bourhis, J. *et al.* Xevinapant or placebo plus chemoradiotherapy in locally advanced squamous cell carcinoma of the head and neck: TrilynX phase III study design. *Future Oncology* https://doi.org/10.2217/fon-2021-1634 (2022) doi:10.2217/fon-2021-1634.

53. Ward, G. A. *et al.* ASTX660, a Novel Non-peptidomimetic Antagonist of cIAP1/2 and XIAP, Potently Induces TNFα-Dependent Apoptosis in Cancer Cell Lines and Inhibits Tumor Growth. *Mol Cancer Ther* **17**, 1381–1391 (2018).

54. Slee, E. A., Adrain, C. & Martin, S. J. Executioner caspase-3, -6, and -7 perform distinct, non-redundant roles during the demolition phase of apoptosis. *J Biol Chem* **276**, 7320–7326 (2001).

55. Nicholson, D. W. *et al.* Identification and inhibition of the ICE/CED-3 protease necessary for mammalian apoptosis. *Nature* **376**, 37–43 (1995).

56. Jan, R. & Chaudhry, G.-S. Understanding Apoptosis and Apoptotic Pathways Targeted Cancer Therapeutics. *Adv Pharm Bull* **9**, 205–218 (2019).

57. Tait, S. W. G. & Green, D. R. Mitochondrial regulation of cell death. *Cold Spring Harb Perspect Biol* **5**, a008706 (2013).

58. Li, P. *et al.* Cytochrome c and dATP-dependent formation of Apaf-1/caspase-9 complex initiates an apoptotic protease cascade. *Cell* **91**, 479–489 (1997).

59. Muzio, M. *et al.* FLICE, A Novel FADD-Homologous ICE/CED-3–like Protease, Is Recruited to the CD95 (Fas/APO-1) Death-Inducing Signaling Complex. *Cell* **85**, 817–827 (1996).

60. Luo, X., Budihardjo, I., Zou, H., Slaughter, C. & Wang, X. Bid, a Bcl2 Interacting Protein, Mediates Cytochrome c Release from Mitochondria in Response to Activation of Cell Surface Death Receptors. *Cell* **94**, 481–490 (1998).

61. Schug, Z. T., Gonzalvez, F., Houtkooper, R. H., Vaz, F. M. & Gottlieb, E. BID is cleaved by caspase-8 within a native complex on the mitochondrial membrane. *Cell Death Differ* **18**, 538–548 (2011).

62. Vince, J. E. *et al.* IAP antagonists target cIAP1 to induce TNFalpha-dependent apoptosis. *Cell* **131**, 682–693 (2007).

63. Du, C., Fang, M., Li, Y., Li, L. & Wang, X. Smac, a mitochondrial protein that promotes cytochrome c-dependent caspase activation by eliminating IAP inhibition. *Cell* **102**, 33–42 (2000).

64. Chang, Y.-C. & Cheung, C. H. A. An Updated Review of Smac Mimetics, LCL161, Birinapant, and GDC-0152 in Cancer Treatment. *Applied Sciences* **11**, 335 (2021).

65. Almuradova, E., Malik, D.-E.-S., Yousaf, S. & Farooqi, A. A. Overview of the progress and prospects of SMAC mimetics in cancers: Is it a silver bullet? *1* **72**, 373–380 (2022).

66. Michie, J., Kearney, C. J., Hawkins, E. D., Silke, J. & Oliaro, J. The Immuno-Modulatory Effects of Inhibitor of Apoptosis Protein Antagonists in Cancer Immunotherapy. *Cells* **9**, 207 (2020).

67. Snacel-Fazy, E. *et al.* SMAC mimetic drives microglia phenotype and glioblastoma immune microenvironment. *Cell Death Dis* **15**, 676 (2024).

68. Beug, S. T. *et al.* Smac mimetics and innate immune stimuli synergize to promote tumor death. *Nat Biotechnol* **32**, 182–190 (2014).

69. Beug, S. T. *et al.* Smac mimetics synergize with immune checkpoint inhibitors to promote tumour immunity against glioblastoma. *Nat Commun* **8**, 14278 (2017).

70. Dobson, C. C. *et al.* Oncolytic virus synergizes with Smac mimetic compounds to induce rhabdomyosarcoma cell death in a syngeneic murine model. *Oncotarget* **8**, 3495–3508 (2017).

71. Morrish, E., Brumatti, G. & Silke, J. Future Therapeutic Directions for Smac-Mimetics. *Cells* **9**, 406 (2020).

72. Baxevanis, C. N., Fortis, S. P. & Perez, S. A. The balance between breast cancer and the immune system: Challenges for prognosis and clinical benefit from immunotherapies. *Seminars in Cancer Biology* **72**, 76–89 (2021).

73. Wu, X. *et al.* Targeting MHC-I molecules for cancer: function, mechanism, and therapeutic prospects. *Mol Cancer* **22**, 194 (2023).

74. Mittal, D., Gubin, M. M., Schreiber, R. D. & Smyth, M. J. New insights into cancer immunoediting and its three component phases — elimination, equilibrium and escape. *Curr Opin Immunol* **27**, 16–25 (2014).

75. Roerden, M. & Spranger, S. Cancer immune evasion, immunoediting and intratumour heterogeneity. *Nat Rev Immunol* **25**, 353–369 (2025).

76. Gubin, M. M. & Vesely, M. D. Cancer Immunoediting in the Era of Immuno-oncology. *Clin Cancer Res* clincanres.1804.2022 (2022) doi:10.1158/1078-0432.CCR-21-1804.

77. Hiam-Galvez, K. J., Allen, B. M. & Spitzer, M. H. Systemic immunity in cancer. *Nat Rev Cancer* **21**, 345–359 (2021).

78. Spitzer, M. H. *et al.* Systemic Immunity Is Required for Effective Cancer Immunotherapy. *Cell* **168**, 487-502.e15 (2017).

79. Man, S. M. & Jenkins, B. J. Context-dependent functions of pattern recognition receptors in cancer. *Nat Rev Cancer* **22**, 397–413 (2022).

80. Liu, Y.-J. Dendritic Cell Subsets and Lineages, and Their Functions in Innate and Adaptive Immunity. *Cell* **106**, 259–262 (2001).

81. Lee, H. K. & Iwasaki, A. Innate control of adaptive immunity: Dendritic cells and beyond. *Seminars in Immunology* **19**, 48–55 (2007).

82. Bern, M. D. *et al.* Inducible down-regulation of MHC class I results in natural killer cell tolerance. *J Exp Med* **216**, 99–116 (2019).

83. Yang, K., Halima, A. & Chan, T. A. Antigen presentation in cancer — mechanisms and clinical implications for immunotherapy. *Nat Rev Clin Oncol* **20**, 604–623 (2023).

84. Coulie, P. G., Van den Eynde, B. J., van der Bruggen, P. & Boon, T. Tumour antigens recognized by T lymphocytes: at the core of cancer immunotherapy. *Nature Reviews Cancer* **14**, 135–146 (2014).

85. Pardoll, D. M. The blockade of immune checkpoints in cancer immunotherapy. *Nat Rev Cancer* **12**, 252–264 (2012).

86. Zhu, L. *et al.* Alginate Particles with Ovalbumin (OVA) Peptide Can Serve as a Carrier and Adjuvant for Immune Therapy in B16-OVA Cancer Model. *Med Sci Monit Basic Res* **23**, 166–172 (2017).

87. Karandikar, S. H. *et al.* Identification of epitopes in ovalbumin that provide insights for cancer neoepitopes. *JCI Insight* **4**, e127882.

88. Basto, A. P. *et al.* Immune response profile elicited by the model antigen ovalbumin expressed in fusion with the bacterial OprI lipoprotein. *Mol Immunol* **64**, 36–45 (2015).

89. Brown, D. M., Fisher, T. L., Wei, C., Frelinger, J. G. & Lord, E. M. Tumours can act as adjuvants for humoral immunity. *Immunology* **102**, 486–497 (2001).

90. Chen, D. S. & Mellman, I. Oncology meets immunology: the cancer-immunity cycle. *Immunity* **39**, 1–10 (2013).

91. Yan, W. & Jiang, S. Immune Cell-Derived Exosomes in the Cancer-Immunity Cycle. *Trends in Cancer* **6**, 506–517 (2020).

92. Chen, D. S. & Mellman, I. Oncology meets immunology: the cancer-immunity cycle. *Immunity* **39**, 1–10 (2013).

93. Pio, R., Ajona, D., Ortiz-Espinosa, S., Mantovani, A. & Lambris, J. D. Complementing the Cancer-Immunity Cycle. *Front. Immunol.* **10**, (2019).

94. Starzer, A. M., Preusser, M. & Berghoff, A. S. Immune escape mechanisms and therapeutic approaches in cancer: the cancer-immunity cycle. *Ther Adv Med Oncol* **14**, 17588359221096219 (2022).

95. Tang, S., Ning, Q., Yang, L., Mo, Z. & Tang, S. Mechanisms of immune escape in the cancer immune cycle. *International Immunopharmacology* **86**, 106700 (2020).

96. Giles, J. R., Globig, A.-M., Kaech, S. M. & Wherry, E. J. CD8+ T cells in the cancer-immunity cycle. *Immunity* **56**, 2231–2253 (2023).

97. Starzer, A. M., Preusser, M. & Berghoff, A. S. Immune escape mechanisms and therapeutic approaches in cancer: the cancer-immunity cycle. *Ther Adv Med Oncol* **14**, 17588359221096219 (2022).

98. Zhu, S. *et al.* Combination strategies to maximize the benefits of cancer immunotherapy. *J Hematol Oncol* **14**, 156 (2021).

99. Emens, L. A. *et al.* Challenges and opportunities in cancer immunotherapy: a Society for Immunotherapy of Cancer (SITC) strategic vision. *J Immunother Cancer* **12**, e009063 (2024).

100. Chen, Y. *et al.* Enhancing cancer immunotherapy: Nanotechnology-mediated immunotherapy overcoming immunosuppression. *Acta Pharmaceutica Sinica B* **14**, 3834–3854 (2024).

101. Hermida-Prado, F. *et al.* Endocrine Therapy Synergizes with SMAC Mimetics to Potentiate Antigen Presentation and Tumor Regression in Hormone Receptor–Positive Breast Cancer. *Cancer Research* **83**, 3284–3304 (2023).

102. Yan, W. & Jiang, S. Immune Cell-Derived Exosomes in the Cancer-Immunity Cycle. *Trends Cancer* **6**, 506–517 (2020).

103. Gurunathan, S., Kang, M.-H., Qasim, M., Khan, K. & Kim, J.-H. Biogenesis, Membrane Trafficking, Functions, and Next Generation Nanotherapeutics Medicine of Extracellular Vesicles. *Int J Nanomedicine* **16**, 3357–3383 (2021).

104. Kuang, L., Wu, L. & Li, Y. Extracellular vesicles in tumor immunity: mechanisms and novel insights. *Mol Cancer* **24**, 45 (2025).

105. Tetta, C., Ghigo, E., Silengo, L., Deregibus, M. C. & Camussi, G. Extracellular vesicles as an emerging mechanism of cell-to-cell communication. *Endocrine* **44**, 11–19 (2013).

106. Abels, E. R. & Breakefield, X. O. Introduction to Extracellular Vesicles: Biogenesis, RNA Cargo Selection, Content, Release, and Uptake. *Cell Mol Neurobiol* **36**, 301–312 (2016).

107. Théry, C. *et al.* Minimal information for studies of extracellular vesicles 2018 (MISEV2018): a position statement of the International Society for Extracellular Vesicles and update of the MISEV2014 guidelines. *J Extracell Vesicles* **7**, 1535750 (2018).

108. Welsh, J. A. *et al.* Minimal information for studies of extracellular vesicles (MISEV2023): From basic to advanced approaches. *Journal of Extracellular Vesicles* **13**, e12404 (2024).

109. Rajagopal, C. & Harikumar, K. B. The Origin and Functions of Exosomes in Cancer. *Front. Oncol.* **8**, (2018).

110. McAndrews, K. M. & Kalluri, R. Mechanisms associated with biogenesis of exosomes in cancer. *Mol Cancer* **18**, 52 (2019).

111. Horbay, R. *et al.* Role of Ceramides and Lysosomes in Extracellular Vesicle Biogenesis, Cargo Sorting and Release. *Int J Mol Sci* **23**, 15317 (2022).

112. Barros, F. M., Carneiro, F., Machado, J. C. & Melo, S. A. Exosomes and Immune Response in Cancer: Friends or Foes? *Front Immunol* **9**, 730 (2018).

113. Nam, G.-H. *et al.* Emerging Prospects of Exosomes for Cancer Treatment: From Conventional Therapy to Immunotherapy. *Adv Mater* **32**, e2002440 (2020).

114. Valencia, K. & Montuenga, L. Exosomes in Liquid Biopsy: The Nanometric World in the Pursuit of Precision Oncology. *Cancers* **13**, 2147 (2021).

115. Xu, Z., Zeng, S., Gong, Z. & Yan, Y. Exosome-based immunotherapy: a promising approach for cancer treatment. *Mol Cancer* **19**, 160 (2020).

116. Huda, M. N. *et al.* Potential Use of Exosomes as Diagnostic Biomarkers and in Targeted Drug Delivery: Progress in Clinical and Preclinical Applications. *ACS Biomater. Sci. Eng.* **7**, 2106–2149 (2021).

117. Yu, D. *et al.* Exosomes as a new frontier of cancer liquid biopsy. *Molecular Cancer* **21**, 56 (2022).

118. Mosquera-Heredia, M. I. *et al.* Exosomes: Potential Disease Biomarkers and New Therapeutic Targets. *Biomedicines* **9**, 1061 (2021).

119. Pando, A., Schorl, C., Fast, L. D. & Reagan, J. L. Tumor Derived Extracellular Vesicles Modulate Gene Expression in T cells. *Gene* **850**, 146920 (2023).

120. Mellman, I., Chen, D. S., Powles, T. & Turley, S. J. The cancer-immunity cycle: Indication, genotype, and immunotype. *Immunity* **56**, 2188–2205 (2023).

121. Hiltbrunner, S. *et al.* Exosomal cancer immunotherapy is independent of MHC molecules on exosomes. *Oncotarget* **7**, 38707–38717 (2016).

122. Richards, K. E. *et al.* Cancer-associated fibroblast exosomes regulate survival and proliferation of pancreatic cancer cells. *Oncogene* **36**, 1770–1778 (2017).

123. Wu, L. *et al.* Exosomes derived from gastric cancer cells activate NF-κB pathway in macrophages to promote cancer progression. *Tumour Biol* **37**, 12169–12180 (2016).

124. van Dommelen, S. M. *et al.* Cetuximab treatment alters the content of extracellular vesicles released from tumor cells. *Nanomedicine (Lond)* **11**, 881–890 (2016).

125. Logozzi, M. *et al.* High levels of exosomes expressing CD63 and caveolin-1 in plasma of melanoma patients. *PLoS One* **4**, e5219 (2009).

126. Riches, A., Campbell, E., Borger, E. & Powis, S. Regulation of exosome release from mammary epithelial and breast cancer cells - a new regulatory pathway. *Eur J Cancer* **50**, 1025–1034 (2014).

127. Aubertin, K. *et al.* Massive release of extracellular vesicles from cancer cells after photodynamic treatment or chemotherapy. *Sci Rep* **6**, 35376 (2016).

128. McAndrews, K. M., Che, S. P. Y., LeBleu, V. S. & Kalluri, R. Effective delivery of STING agonist using exosomes suppresses tumor growth and enhances antitumor immunity. *J Biol Chem* **296**, 100523 (2021).

129. Li, Z. *et al.* Exosomal miRNA-16-5p Derived From M1 Macrophages Enhances T Cell-Dependent Immune Response by Regulating PD-L1 in Gastric Cancer. *Front Cell Dev Biol* **8**, 572689 (2020).

130. Hansen, A. S. *et al.* T-cell derived extracellular vesicles prime macrophages for improved STING based cancer immunotherapy. *J Extracell Vesicles* **12**, e12350 (2023).

131. Gardiner, C., Ferreira, Y. J., Dragovic, R. A., Redman, C. W. G. & Sargent, I. L. Extracellular vesicle sizing and enumeration by nanoparticle tracking analysis. *J Extracell Vesicles* **2**, (2013).

132. Welsh, J. A. *et al.* Minimal information for studies of extracellular vesicles (MISEV2023): From basic to advanced approaches. *J Extracell Vesicles* **13**, e12404 (2024).

133. Inaba, K. *et al.* The tissue distribution of the B7-2 costimulator in mice: abundant expression on dendritic cells in situ and during maturation in vitro. *J Exp Med* **180**, 1849–1860 (1994).

134. Winzler, C. *et al.* Maturation Stages of Mouse Dendritic Cells in Growth Factor–dependent Long-Term Cultures. *J Exp Med* **185**, 317–328 (1997).

135. Yamashita, I., Nagata, T., Tada, T. & Nakayama, T. CD69 cell surface expression identifies developing thymocytes which audition for T cell antigen receptor-mediated positive selection. *Int Immunol* **5**, 1139–1150 (1993).

136. Agata, Y. *et al.* Expression of the PD-1 antigen on the surface of stimulated mouse T and B lymphocytes. *Int Immunol* **8**, 765–772 (1996).

137. Barber, D. L. *et al.* Restoring function in exhausted CD8 T cells during chronic viral infection. *Nature* **439**, 682–687 (2006).

138. Bentin, J., Vaughan, J. H. & Tsoukas, C. D. T cell proliferation induced by anti-CD3 antibodies: requirement for a T-T cell interaction. *Eur J Immunol* **18**, 627–632 (1988).

139. Inaba, K. *et al.* Isolation of dendritic cells. *Curr Protoc Immunol* **Chapter 3**, 3.7.1-3.7.19 (2009).

140. Petersen, S. L. *et al.* Autocrine TNFalpha signaling renders human cancer cells susceptible to Smac-mimetic-induced apoptosis. *Cancer Cell* **12**, 445–456 (2007).

141. Petersen, S. L., Peyton, M., Minna, J. D. & Wang, X. Overcoming cancer cell resistance to Smac mimetic induced apoptosis by modulating cIAP-2 expression. *Proc Natl Acad Sci U S A* **107**, 11936–11941 (2010).

142. Hao, Q. & Tang, H. Interferon-γ and Smac mimetics synergize to induce apoptosis of lung cancer cells in a TNFα-independent manner. *Cancer Cell Int* **18**, 84 (2018).

143. Yu, X., Harris, S. L. & Levine, A. J. The regulation of exosome secretion: a novel function of the p53 protein. *Cancer Res* **66**, 4795–4801 (2006).

144. Yu, X., Harris, S. L. & Levine, A. J. The regulation of exosome secretion: a novel function of the p53 protein. *Cancer Res* **66**, 4795–4801 (2006).

145. van der Pol, E. *et al.* Particle size distribution of exosomes and microvesicles determined by transmission electron microscopy, flow cytometry, nanoparticle tracking analysis, and resistive pulse sensing. *Journal of Thrombosis and Haemostasis* **12**, 1182–1192 (2014).

146. Ostrowski, M. *et al.* Rab27a and Rab27b control different steps of the exosome secretion pathway. *Nat Cell Biol* **12**, 19–30; sup pp 1-13 (2010).

147. Essandoh, K. *et al.* Blockade of exosome generation with GW4869 dampens the sepsis-induced inflammation and cardiac dysfunction. *Biochim Biophys Acta* **1852**, 2362–2371 (2015).

148. Granqvist, V., Holmgren, C. & Larsson, C. Induction of interferon-β and interferon signaling by TRAIL and Smac mimetics via caspase-8 in breast cancer cells. *PLoS One* **16**, e0248175 (2021).

149. Lalaoui, N. *et al.* Targeting triple-negative breast cancers with the Smac-mimetic birinapant. *Cell Death Differ* **27**, 2768–2780 (2020).

150. Allensworth, J. L., Sauer, S. J., Lyerly, H. K., Morse, M. A. & Devi, G. R. Smac mimetic Birinapant induces apoptosis and enhances TRAIL potency in inflammatory breast cancer cells in an IAP-dependent and TNF-α-independent mechanism. *Breast Cancer Res Treat* **137**, 359–371 (2013).

151. Jin, G. *et al.* Smac mimetic-induced caspase-independent necroptosis requires RIP1 in breast cancer. *Molecular Medicine Reports* **13**, 359–366 (2016).

152. Jiang, X., Shen, C., Rey-Ladino, J., Yu, H. & Brunham, R. C. Characterization of Murine Dendritic Cell Line JAWS II and Primary Bone Marrow-Derived Dendritic Cells in Chlamydia muridarum Antigen Presentation and Induction of Protective Immunity. *Infection and Immunity* **76**, 2392–2401 (2008).

153. Düchler, M. *et al.* Melanoma-Derived Extracellular Vesicles Bear the Potential for the Induction of Antigen-Specific Tolerance. *Cells* **8**, 665 (2019).

154. Granqvist, V., Holmgren, C. & Larsson, C. Induction of interferon-β and interferon signaling by TRAIL and Smac mimetics via caspase-8 in breast cancer cells. *PLoS One* **16**, e0248175 (2021).

155. Müller-Sienerth, N. *et al.* SMAC Mimetic BV6 Induces Cell Death in Monocytes and Maturation of Monocyte-Derived Dendritic Cells. *PLOS ONE* **6**, e21556 (2011).

156. Hao, S. *et al.* Mature dendritic cells pulsed with exosomes stimulate efficient cytotoxic T-lymphocyte responses and antitumour immunity. *Immunology* **120**, 90–102 (2007).

157. Simms, P. E. & Ellis, T. M. Utility of flow cytometric detection of CD69 expression as a rapid method for determining poly- and oligoclonal lymphocyte activation. *Clin Diagn Lab Immunol* **3**, 301–304 (1996).

158. Clutton, G. T. *et al.* CD3 downregulation identifies high-avidity human CD8 T cells. *Clin Exp Immunol* **215**, 279–290 (2024).

159. Agata, Y. *et al.* Expression of the PD-1 antigen on the surface of stimulated mouse T and B lymphocytes. *Int Immunol* **8**, 765–772 (1996).

160. Alsaab, H. O. *et al.* PD-1 and PD-L1 Checkpoint Signaling Inhibition for Cancer Immunotherapy: Mechanism, Combinations, and Clinical Outcome. *Front Pharmacol* **8**, 561 (2017).

161. Barber, D. L. *et al.* Restoring function in exhausted CD8 T cells during chronic viral infection. *Nature* **439**, 682–687 (2006).

162. Burton, A. M., Ligman, B. R., Kearney, C. A. & Murray, S. E. SMAC mimetics inhibit human T cell proliferation and fail to augment type 1 cytokine responses. *Cellular Immunology* **384**, 104674 (2023).

163. Kim, D.-S. *et al.* Smac mimetics and oncolytic viruses synergize in driving anticancer T-cell responses through complementary mechanisms. *Nat Commun* **8**, 344 (2017).

164. Bhanpattanakul, S. *et al.* Modulation of MHC expression by interferon-gamma and its influence on PBMC-mediated cytotoxicity in canine mast cell tumour cells. *Sci Rep* **14**, 17837 (2024).

165. Yang, M. *et al.* Interferon regulatory factor 1 priming of tumour-derived exosomes enhances the antitumour immune response. *Br J Cancer* **118**, 62–71 (2018).

166. MacNabb, B. W. *et al.* Dendritic cells can prime anti-tumor CD8+ T cell responses through major histocompatibility complex cross-dressing. *Immunity* **55**, 982-997.e8 (2022).

167. Wolfers, J. *et al.* Tumor-derived exosomes are a source of shared tumor rejection antigens for CTL cross-priming. *Nat Med* **7**, 297–303 (2001).

168. Sun, H. *et al.* Design of Small-Molecule Peptidic and Non-Peptidic Smac Mimetics. *Acc Chem Res* **41**, 1264–1277 (2008).

169. Bai, L., Smith, D. C. & Wang, S. Small-molecule SMAC mimetics as new cancer therapeutics. *Pharmacology & Therapeutics* **144**, 82–95 (2014).

170. Chang, Y.-C. & Cheung, C. H. A. An Updated Review of Smac Mimetics, LCL161, Birinapant, and GDC-0152 in Cancer Treatment. *Applied Sciences* **11**, 335 (2021).

171. Badovinac, V. P., Haring, J. S. & Harty, J. T. Initial T cell receptor transgenic cell precursor frequency dictates critical aspects of the CD8(+) T cell response to infection. *Immunity* **26**, 827–841 (2007).

172. Wahlund, C. J. E. *et al.* Exosomes from antigen-pulsed dendritic cells induce stronger antigen-specific immune responses than microvesicles in vivo. *Sci Rep* **7**, 17095 (2017).

173. Bu, N. *et al.* Exosome-loaded dendritic cells elicit tumor-specific CD8+ cytotoxic T cells in patients with glioma. *J Neurooncol* **104**, 659–667 (2011).

174. Hao, S., Bai, O., Yuan, J., Qureshi, M. & Xiang, J. Dendritic cell-derived exosomes stimulate stronger CD8+ CTL responses and antitumor immunity than tumor cell-derived exosomes. *Cell Mol Immunol* **3**, 205–211 (2006).

175. Hao, S. *et al.* Mature dendritic cells pulsed with exosomes stimulate efficient cytotoxic T-lymphocyte responses and antitumour immunity. *Immunology* **120**, 90–102 (2007).

176. Blanchard, N. *et al.* TCR activation of human T cells induces the production of exosomes bearing the TCR/CD3/zeta complex. *J Immunol* **168**, 3235–3241 (2002).

177. Seo, N. *et al.* Activated CD8+ T cell extracellular vesicles prevent tumour progression by targeting of lesional mesenchymal cells. *Nat Commun* **9**, 435 (2018).

178. Fu, W. *et al.* CAR exosomes derived from effector CAR-T cells have potent antitumour effects and low toxicity. *Nat Commun* **10**, 4355 (2019).

179. Wolfers, J. *et al.* Tumor-derived exosomes are a source of shared tumor rejection antigens for CTL cross-priming. *Nat Med* **7**, 297–303 (2001).

180. Wang, R., Zhu, T., Hou, B. & Huang, X. An iPSC-derived exosome-pulsed dendritic cell vaccine boosts antitumor immunity in melanoma. *Mol Ther* **31**, 2376–2390 (2023).